Sensitivity and Uncertainty Quantification of Transition Scenario Simulations

Nuclear Fuel Cycle and Supply Chain

EXECUTIVE SUMMARY

This report documents the first collective attempt at developing and applying capabilities to quantify uncertainties, assess parametric sensitivities, and optimize multiple parameters and metrics in fuel cycle simulations generated by the SA&I Campaign. To do this, external codes that were designed to perform sensitivity analysis and uncertainty quantification (SA&UQ) needed to be coupled to the SA&I Campaign's nuclear fuel cycle simulators (NFCS). In FY20, two approaches were pursued: 1) coupling Cyclus to an ORNL-internal code called MOT (Metaheuristic Optimization Tool) and 2) coupling DYMOND to the open-source SA&UQ tool kit Dakota.

The primary objective of having these NFCS/SA&UQ coupled capabilities is to better inform DOE-NE and other stakeholders on the results generated from the NFCS. For a given set of fuel cycle strategies, policies, and technology assumptions that make up a fuel cycle scenario, these NFCS have traditionally been used by the SA&I Campaign to provide quantitative answers in terms of year-by-year mass flows, infrastructure requirements, costs, *etc.* With these newly developed coupled capabilities, the SA&I Campaign can now efficiently simulate hundreds or thousands of these scenarios, sample large ranges of parameters and assumptions, and use the unique features of the SA&UQ tools to process the data. This enables providing answers with known and propagated uncertainties, determining the sensitivity of important metrics to different parameters and assumptions, quantifying how much fuel cycle and technology parameters impact each other, and producing optimized fuel cycle strategies for single and multiple variables.

To demonstrate these new capabilities, the Cyclus/MOT was used to model several scenarios ranging from simple fleet retirements to transitions to advanced reactors. Specifically, for a transition scenario from LWRs to SFRs and advanced LWRs, uncertainty quantification, sensitivity analysis, and optimization studies were applied to cases involving single and multiple parameter (input) and single and multiple metric (output) variations. In addition, a similar transition scenario was modeled to demonstrate how to optimize the reprocessing capacity parameter to minimize two performance metrics while taking into account uncertainties from two other parameters. Lastly, a depletion module based on SCALE/ORIGEN was added in Cyclus to simulate the third scenario that was designed to quantify the impact of the modeling assumption that all LWR used nuclear fuel have the same burnup.

The newly developed DYMOND/Dakota capability was also applied to a transition scenario from the existing fleet to small modular reactors and fast reactors. This particular scenario involves not only explicit isotopic depletion via ORIGEN-2, but also includes multirecycling and utilizing the criticality search feature to determine the fresh fuel composition of recycled fuel, a feature unique to the DYMOND NFCS. A large database of simulations were run with 4 main parameters that were sampled: start date of reprocessing, reprocessing capacity, energy demand growth rate, and advanced reactor share of the fleet. The 4 main metrics were uranium consumption, enrichment requirements, waste generation, and levelized cost of electricity using data from the Cost Basis Report. The demonstrated SA&UQ results include those that inform on how to choose parameters to avoid "failed" scenarios, Sobol' indices that inform on the importance of various parameters individually and synergistically, and Analysis of Variance (ANOVA) studies that decompose parameter ranges into groups and informs on whether variations are statistically significant.

CONTENTS

TABLES

FIGURES

SYSTEMS ANALYSIS & INTEGRATION CAMPAIGN

SENSITIVITY AND UNCERTAINTY QUANTIFICATION OF TRANSITION SCENARIO SIMULATIONS

1.   Introduction

The nuclear fuel cycle is a complicated system with many feedback mechanisms that can have unintuitive effects when transitioning between fuel cycle systems. Nuclear Fuel Cycle Simulators (NFCS) or colloquially referred to as "fuel cycle systems codes" are often used to perform fuel cycle simulations, including scenarios of reactor deployment or fuel cycle transition, to capture these complex dynamics and relationships to provide quantitative feedback to stakeholders and decision makers on the impacts of various fuel cycle strategies, policies, and scenarios. Over the past several years, the Systems Analysis & Integration (SA&I) Campaign has leveraged several NFCS (Cyclus, DYMOND, ORION, VISION, *etc.*) to produce important scenario results to inform DOE-NE on the benefits and drawbacks of various pathways to the most promising fuel cycles.

However, these fuel cycle simulations have three major sources of uncertainty – parametric, structural, and algorithmic, and until now, these uncertainties have not been properly quantified as part of their results:

1) <u>Parametric uncertainties</u> are essentially uncertainties in the input value to a fuel cycle scenario simulation, such as future nuclear energy demand (in TWe-h/year) or the date when advanced fast reactors start generating commercial electricity on a large scale. Some parameters are impossible to know or there is insufficient information to know with absolute certainty. Thus, a range of parameter values are used in many simulations as part of uncertainty quantification.

2) <u>Structural uncertainties</u> are also known as model inadequacy or bias. These uncertainties result from known and intentional approximations made to the model or "structure". Such approximations may include modeling reactors with constant refueling and operational time, or in some cases, not modeling the burnup difference between start-up core and the steady-state core.

3) <u>Algorithmic uncertainties</u> are also known as numerical uncertainties and are more related to the specific calculations or mathematical/physics algorithms used to generate quantitative results. An example of this in NFCS is the modeling of fuel depletion. The sources of the uncertainties are much harder to isolate in these complex physics models and numerical methods since they could be a combination of many algorithmic approximations.

The focus of the work presented in this report is primarily on addressing the <u>parametric uncertainties</u>. The structural and algorithmic uncertainties will be assessed in more detail in future work. It should be noted that the impacts of algorithmic uncertainties were assessed in various code-to-code comparisons of fuel cycle simulators including ones performed in previous years by the SA&I Campaign. However, these algorithmic uncertainties were not specifically emphasized at the time.

To better understand the models that are being simulated and the result of these uncertainties, sensitivity analysis and uncertainty quantification (SA&UQ) are performed. These approaches reveal how the system performance changes as either a single or group of uncertain parameters change. This relationship is studied through sampling methods and surrogate models to calculate a distribution on system performance measures (*i.e.*, response metrics) and to understand which parameters contribute most to the variance of the response and the synergistic relationships between parameters.

To perform these SA&UQ studies efficiently, the SA&I campaign's fuel cycle codes needed to be coupled to external tools that were designed for SA&UQ calculations. Two approaches were pursued in parallel for this year's work: coupling Cyclus with the Metaheuristic Optimization Tool (MOT) developed at ORNL and interfacing DYMOND (DYnamic MOdel of Nuclear Deployment) with Dakota (Design Analysis Kit for Optimization and Terascale Application).

Section 2 briefly describes each of the NFCS (Cyclus and DYMOND), followed by the SA&UQ tools (MOT and Dakota) and their combined/coupled capabilities (Cyclus/MOT, DYMOND/Dakota) that were developed as part of this year's work.

Section 3 describes three simplified scenarios that were simulated using the Cyclus/MOT tool to demonstrate its capability to perform uncertainty quantification, sensitivity analysis, and optimization on single variable and multi-variable parametric studies. This also served to demonstrate that Cyclus was successfully utilized by national laboratory staff for production-level calculations.

Section 4 describes DYMOND/Dakota simulations based on a partial transition scenario to Gas-cooled Fast Reactors that were performed to demonstrate the newly developed multi-dimensional sensitivity analysis capabilities such failure space assessment, Sobol' indices, and Analysis of Variance (ANOVA). In particular, this scenario involved multi-recycling of fuel that required utilizing DYMOND's new depletion-based "criticality search" feature to update the loaded fuel isotopics.

Section 5 summarizes the general conclusions from this study.

In addition, a Graphical User Interface (GUI) for Cyclus was developed by ORNL help non-developers generate input and execute Cyclus remotely. This approach greatly facilitated the usability of Cyclus since it removed the code installation and build requirements that have been significant barriers for new users and allowed inputs to be generated using traditional operating systems like Windows. This GUI is described in Appendix A.

2.   Background

To develop and assess the campaign's capabilities to perform SA&UQ calculations based on the results of NFCS, two pathways were chosen this year to enable the multi-laboratory teams to build experience and leverage unique features from two different code systems that will benefit future analyses. The ORNL team pursued the Cyclus/MOT approach while the ANL team pursued the DYMOND/Dakota approach.

2.1   Nuclear Fuel Cycle Simulator Descriptions

2.1.1   Cyclus

Cyclus [Huff *et al.,* 2016] is an agent-based system level fuel cycle simulator developed by universities through multiple Nuclear Energy University Programs (NEUPs). Cyclus was designed to be open source and modular in order to facilitate collaboration between multiple universities and institutions for development and applications. The project is maintained and developed by a voluntary developer team consisting of university faculty, postdoctoral research staff, and graduate students at various institutions. It has been six years since the initial release of Cyclus, and numerous validation studies [Bae *et al.,* 2019, ORNL 2019, Djokic *et al.,* 2015, Gidden *et al.,* 2012] demonstrated Cyclus' competence as a dynamic NFCS.

Based on the Cyclus user feedback survey conducted by the SA&I Campaign in FY19 [ORNL 2019], the primary barriers to new users were the relatively complex installation and build procedure for the code, input generation, output parsing, and outdated documentation. To address these challenges, a Graphical User Interface (GUI) was developed by ORNL that can be executed via MacOS or Windows and connects to an already compiled version of Cyclus hosted on a Cloud system. This remote access feature eliminates the most problematic barrier to entry which is installation and building of the code on a local system. In addition, the input generation and output processing is simplified with buttons and pop-up instructional guides to help new users. The GUI was tested and appraised by the ANL and INL team members who were not involved in the GUI development. They were able to set up their own inputs and execute them successfully using this GUI, which also helped them fully appreciate how the agent-based code was intended to operate (setting up the agent-based problem and letting the dynamic resource exchange module guide the evolution of the scenario). Having non-developers set up, execute, and post process a working scenario in Cyclus, thanks to the GUI, greatly helped the new users understand the full potential of Cyclus. Since the GUI was meant to be an interactive learning tool, it does not enable utilizing all of the features of Cyclus. The hope is to train new users on the GUI and transition them to generating inputs in the native XML format which enables the flexibility to generate much more complex scenarios. Additional information on the GUI is provided in Appendix A.

2.1.2   DYMOND

DYMOND [ANL 2019] is an Argonne National Laboratory developed and maintained NFCS first developed in 2001. The DYMOND code models the nuclear fuel cycle through a hybrid modeling of paradigms, combining system dynamics, discrete event, and agent-based modeling in the AnyLogic modeling platform (switched over from Stella in 2019) and depletion physics through coupling with ORIGEN2 (also added in 2019). The work flow of DYMOND uses these different paradigms to manage the abstraction level of the nuclear fuel cycle. Material flows, transport, and head-end processes are modeled as stocks and flows within a system with feedback mechanisms dictated by the higher definition agents. Agent models are used for the reactors and reprocessing with discrete event models dictating their construction, operational state, and decommissioning. The model is organized in this manner to mirror the level of granularity needed when studying potential benefits of technologies or policies on hypothetical fuel cycles. The preserved component linking the model abstraction levels is the composition of the materials at key locations in the fuel cycle – at

reactor facilities in the core, in spent fuel storage, at reprocessing plants, in separated storage, and material that is in storage awaiting or in final disposal.

DYMOND explicitly tracks 25 nuclides – actinides that have the greatest impact on fuel recycling in advanced reactor concepts – and currently a lumped material composite of all fission products. The transmutation of nuclear fuel in a reactor is calculated using pre-generated reactor-specific depletion libraries in ORIGEN2. These calculations determine the fuel composition after irradiation and cooling from a reactor based on the reactor power and cycle specifications. Decay of materials in all parts of the fuel cycle is also accounted for through a simplified Bateman equation solver for the explicitly tracked nuclides that recalculates material compositions at each month of the simulation. The coupling of ORIGEN also allows for a more advanced feature – determination of fresh fuel composition requirements through a criticality search – as an alternative to the commonly used fuel "recipes" or approximate nuclide reactivity worth (*i.e.*, Pu239 equivalence). This feature allows to more accurately determine fuel requirements from reprocessed material streams for a wider range of reactor designs with material-stream composition feedback mechanisms and minimal approximations. Though the use of these more physically accurate modeling capabilities is more computationally expensive, DYMOND has been made compatible with both concurrent execution and multiple-processor parallelism to off-set the computational cost.

2.2   SA&UQ Tool Descriptions

2.2.1   MOT

Metaheuristic Optimization Tool (MOT) is an in-house code developed by ORNL to be a general optimization and sampling driver [Variansyah *et al.*, 2020]. It consists of 3 major Python classes collected in the Python MOT package: Perturber, Fitter, and Method. MOT can be obtained from the following Git repository: https://code.ornl.gov/ybb/MOT.git. The repository is currently accessible to people with an invitation, but is planned to be openly accessible in the near future.

The manner in which the objects are connected when performing optimization is depicted in Figure 1. Users define the optimization problem by supplying descriptions of each search variable in Perturber and supplying user-defined <Simulation> and <Function> objects into Fitter. Then, users supply the set up Perturber and Fitter into the Method. The parameters of these objects may need to be set up before they are entered. Finally, Method solves the optimization problem described by the Perturber and Fitter, resulting in the optimum variable set. In other words, Method governs what the Perturber sends to the Fitter, and from what Method receives from Fitter, it sends new values to the Perturber, until a user-defined exit condition has been met.
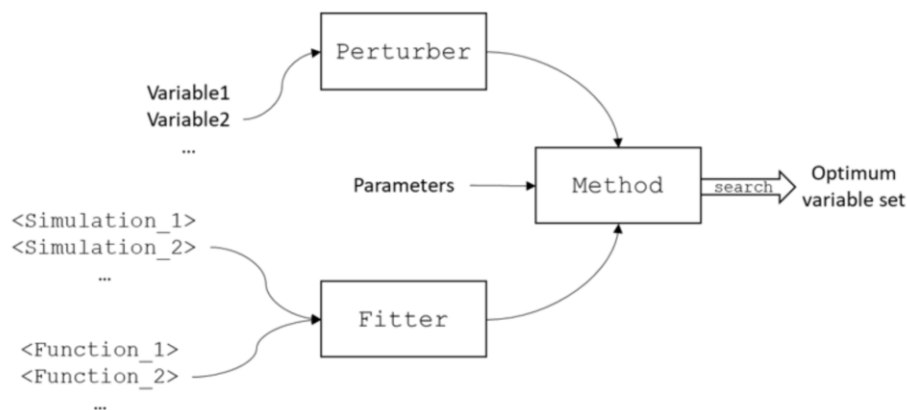

Figure 1 Flowchart of MOT communication between modules and optimization.

2.2.1.1   *Cyclus/MOT Coupled Approach*

In this work utilizing Cyclus with MOT, the Perturber would be set with the minimum and maximum values of the parameters to be perturbed. The Fitter object would have functions that take the parameters, create a Cyclus input, run Cyclus, and parse the Cyclus output to obtain the metrics. The Method object would contain either a sampler, which samples the parameters given a user-defined distribution, or an optimization algorithm. The optimization algorithm used for this work is a non-dominated sorting genetic algorithm 2 (NSGA-II) [Deb *et al.,* 2002], a multi-objective, multivariate elitist genetic optimization algorithm.

A genetic optimization algorithm is a method for solving an optimization problem based on a natural process that mimics biological evolution. The algorithm takes an initial random population, and modifies the population given its fitness (metric). It takes the better performing population set and uses them to create the next generation, through crossover and random mutation. Crossover is when certain features (that are considered to yield good fitness) are taken from a population to move on to the next generation. Random mutation is when a feature of a population in the next generation is randomly perturbed, so that a wider parameter space can be explored.

A genetic algorithm is set with two important user-defined parameters - number of generations and populations per generation. For our applications in this work, we consider "populations" in terms of number of unique simulations. These parameters are called hyperparameters, in order to differentiate from simulation parameters (such as LWR operating lifetime). For each generation, the defined number of populations (simulations) are run, and with the evaluated population metrics, the optimization algorithm generates the next generation, to yield better population metrics (*i.e.*, evolve). The process, in the context of this report, can be described in the following steps:

1. Randomly generate *N* (population per generation parameter) Cyclus input files, by sampling from a user-defined range of input parameters.

2. Run Cyclus on the *N* files.

3. Postprocess output files from each simulation (population) to obtain metrics.

4. Optimization algorithm evaluates the metrics from each population, and generates next generation of *N* input files (populations).

5. Repeat the above steps for the user-defined number of generations.

For example, if we set the metric that scenarios that yield lower nuclear waste are better or "more fit", then having higher amounts of fast reactors that recycle their own fuel considered a 'good' feature for scenarios. Therefore, the populations of scenarios with large amounts of fast reactors in the system will 'pass on' this feature to the next generation (*i.e.*, the next set of simulations). Thus, in future generations, the larger part of the population would have large fast reactor fleets, since the populations with no or few fast reactors have 'died off'. This causes the future generations to be closer to an optimal (or 'fittest') population.

2.2.2   **Dakota**

Dakota (Design Analysis Kit for Optimization and Terascale Application) [Adams *et al.,* 2019] is a standardized toolkit developed by Sandia National Laboratory for optimization, global sensitivity and variance analysis, parameter estimation, uncertainty quantification, and verification. Dakota is designed as an ease-of-use tool for interfacing optimization and analysis methods with a wide range of engineering software under otherwise difficult conditions. These difficult problems include those that adopt meta-level strategies such as surrogate models and hybrid-optimization or multi-level parallelism. It is thanks to this design that advanced modeling techniques can be used in this study to overcome difficulties that arise in NFCS such as

computationally expensive simulations that include both time-dependent system evolution and evolution of the fuel compositions through depletion, decay, and other physics. The DYMOND/Dakota application in this study was performed through the use of surrogate models (a quadratic regression and Gaussian process model) trained on sampling a massive amount of data generated from DYMOND. Dakota is publicly released and available through Sandia at dakota.sandia.gov.

The main classes of problems that Dakota is designed to solve are parameter studies, design of experiment, uncertainty quantification, optimization, and calibration. This effort makes use of two of these classes – parameter studies via joint variation on a multidimensional grid and design of experiment via a Design and Analysis of Computer Experiment (DACE) study to generate global sensitivity measures. The approach to these two problems are similar in that they explore parametric changes within the NFCS model by the resultant response data set in the parameter space using Monte Carlo sampling methods (Latin Hypercube Sampling for the parametric studies, and Orthogonal Array Sampling for the DACE studies).

In both problems, the goal is the same – to use sensitivity analysis techniques to identify which of the design parameters have the most influence on the response quantities. This information is useful as both an assessment of the behavior of response functions as well as a preliminary step in the optimization of a model by limiting the parameter space that needs to be explored. For this work two of the available measures for sensitivity analysis in Dakota were chosen: Sobol' indices from the parametric study and Analysis of Variance (ANOVA) analysis through DACE. Sobol' indices and ANOVA analysis both provide a global, as opposed to local, measure of the importance of parameters. However, Sobol' indices provide a greater quantification of synergistic effects, whereas the multi-dimensional ANOVA analysis is a more conventional method with several statistical tests for result verification.

2.2.2.1   *DYMOND/Dakota Coupled Approach*

In Dakota, an interface is what defines a function evaluation or response creation but is otherwise considered a black-box. The DYMOND/Dakota coupling scheme developed in this work has Dakota act as the driver, generating the parameter inputs and managing either the serial or parallel execution of the interface, whether that be the DYMOND model or a data-generated surrogate model, through execution and wait commands on a generated independent process. The interface that was created to allow Dakota to interact with DYMOND makes use of the Dakota interfacing Python module and a DYMOND-native distributed file system. The Python module simplifies the interaction with Dakota parameter and result files by managing the construction and syntax, and the DYMOND-native file system allows for data preservation and simulation modularity. These two features allow for the study to be quickly and easily repeated in case of changes in response evaluations or simulation/calculation errors that require restarting or repeating.

The coupling is coded in Python and managed through a set of system calls to execute the DYMOND simulation and two modules. The first module takes the parameters from Dakota and then edits a base scenario Excel-Based DYMOND input to match the behavior of each parameter described in Section 4.1.1. This module uses a Windows client built-in to Python to force the built-in Excel functions to update all cell references and calculated input values. The second module is for the analysis of the DYMOND output and calculation of the response metrics (see Section 4.1.2) that are returned to Dakota and are associated with the parameter set. Also included in the interface is a system for ensuring unique execution of each DYMOND simulation and unified storage of all cases' inputs and outputs.

3.   Cyclus/MOT Results

For the Cyclus/MOT calculations, three different scenarios were set up to test various capabilities. Scenario 1 is a simple transition scenario from existing LWRs to advanced LWRs (SMRs and AP1000s) and Gen-IV sodium-cooled fast reactors. Many instances of this scenario were generated via Cyclus to allow MOT to demonstrate its SA&UQ features for example cases: a multi-parameter (input)/single-metric (output) uncertainty quantification, a single parameter/single metric sensitivity analysis, and a multi-parameter/multi-metric optimization. Scenario 2 is very similar to Scenario 1 but with a few changes to allow demonstration of a more complex calculation: optimizing one parameter to minimize two metrics while considering the uncertainties in two other parameters. Scenario 3 is an additional single parameter uncertainty quantification but applied to a scenario that includes fuel depletion rather than using recipes in Cyclus.

3.1   Scenario 1: Base Case

We first chose a base-case scenario, where the U.S. nuclear fleet is transitioned into a fleet of Gen-III LWRs, namely Small Modular Reactor (SMR) [Ingersoll *et al.,* 2014] or AP1000 Pressurized Water Reactors (AP1000) [Schulz 2006], followed by a partial transition with Gen-IV reactors. The Gen-IV reactor chosen is the Advanced Burner Reactor (ABR) [Kim *et al.,* 2009], which is a Sodium-cooled Fast Reactor (SFR) that 'burns' minor actinides to reduce high level waste (HLW) long-term radiotoxicity and decay heat. The ABR uses fuel made from recycled TRU from the existing LWRs and Gen-III LWRs; there is no multirecycling of ABR fuel for simplicity. Hence, the recipe approach (charge and discharge compositions pre-calculated using external physics tools) to simulate fuel evolution is applicable. Reprocessing of LWR fuel is unconstrained (as needed). The nuclear power demand in the U.S. is shown in Figure 2.
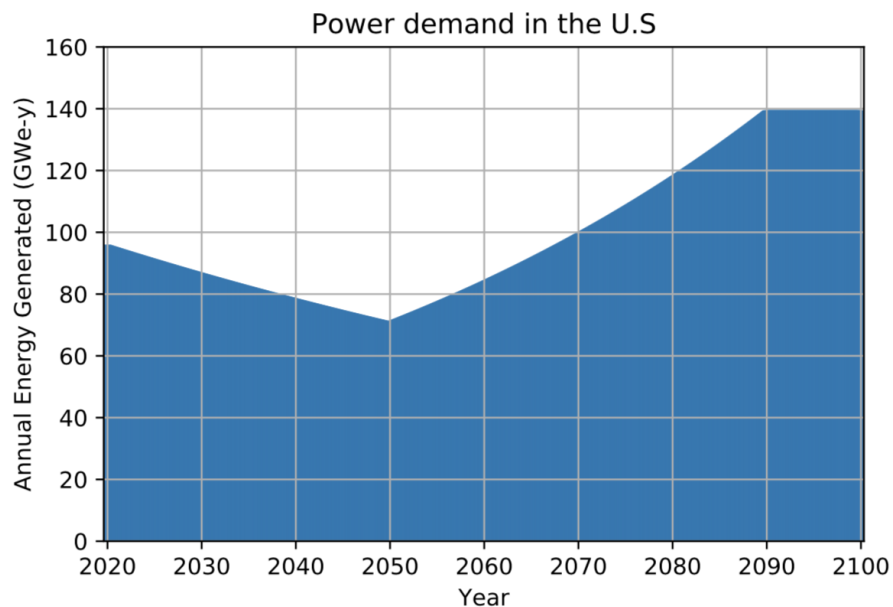

Figure 2 The assumed nuclear power demand for Cyclus/MOT scenarios

The initial fleet of ≈100 reactors is gradually retired from 2020 to shortly after 2050. To make up for the power demand, Gen-III LWRs (SMRs and AP1000s) are deployed. In year 2040 and 2045, advanced reactor prototypes are to be deployed, and from 2050, the reactors are deployed so that 10% of the new reactors are ABRs.

3.1.1   Uncertainty Quantification (Multi-Parameter / Single Metric)

Given this scenario, we chose three parameters to perturb:

1. Legacy reactor lifetime extension [0, 20 years]

2. New Gen-III Light Water Reactors' (LWRs) lifetime [60, 80 years]

3. Fraction of SMRs in new Gen-III LWRs [0, 1] (*i.e.*, 1 means only SMRs are deployed)

and a single metric:

1. LWR UNF discharged from 2020 to 2100 in tons of initial heavy metal (TiHM)

The parameters and the metric are intentionally chosen to produce intuitive results. The metric focuses on LWR UNF discharged for simplicity; ABR discharged fuel would be another potential metric. The fraction of SMRs in new Gen-III LWRs deployed will cause an increase in the LWR UNF metric, since SMR fuels have a lower burnup, leading to a lower uranium utilization (*i.e.*, energy generated per uranium). Table 1 compares an AP1000 with 20 SMRs that provide the same amount of electric power. The total fuel per electric energy was calculated by dividing the amount of fuel per batch by the power capacity multiplied by cycle time. Assuming the same refueling outage duration, the AP1000 has a lower capacity factor than the SMRs, but that does not affect burnup.

Table 1 LWR specifications

Reactor parameters	AP1000	20 SMRs	Legacy PWR*
Thermal Power [MWth]	3,000	3,000	3,000
Electric Power [MWe]	1,000	1,000	1,000
Assembly Mass [kg]	446	249.76	446
Num. Assemblies in core	193	740	193
Cycle time [days]	480	720	360
Number of batches	3	3	3
Burnup [MWth day /MTHM]	50,187	35,060	37,640
Total fuel / energy [kg / MWe day]	0.0597	0.0855	0.0797
*Legacy PWR specifications are linearly scaled with reactor power capacity from the PRIS database.			

The increase in legacy reactors' lifetime should not have a large impact on the metric, unless they increase the number of reactors deployed in the simulation. Reactor deployment in the simulation causes an increase in the total UOX waste because there is more start-up core loaded into reactors, which are more than the refueling batches. The same logic can be applied to the Gen-III LWR lifetime. If it does not cause an increase in the number of reactors deployed, it should not have a dramatic effect on the metric.

We created 200 simulations of the base case scenario (Scenario 1) by randomly selecting from a uniform distribution of the three parameters. The total runtime was 71 minutes using the Cyclus/MOT coupled approach. Figure 3 shows the histograms of the three parameters (shown in blue) and the metric (shown in red). The distributions of the sampled parameters are pretty wide and do appear random/uniform. Increasing the population of simulations from 200 to over 1000 or more may yield a flatter shape of the parameter distributions or a smoother bell-curve shape for the metric distribution. In other words, more samples would be need for better assessment of the distribution types. Regardless, the statistics of the results are shown in Table 2. The mean value of the metric is about 165,000 TiHM of LWR UNF generated

during the scenario with a standard deviation (statistical uncertainty) of about 20,000 TiHM. This means that given uniform sampling of the 3 different parameters and their many resulting combinations (200 simulations), the end result for the metric will be 165,000 +/- 20,000 TiHM of LWR UNF generated. Being able to add this additional uncertainty in a value calculated from a NFCS is a significant achievement for the SA&I Campaign as parametric uncertainties are prevalent in NFCS. The goal of NFCS is to assess resource distribution and help inform on policy decisions, therefore providing this range of potential outcomes along with the statistics allows for a more informed and robust decision.
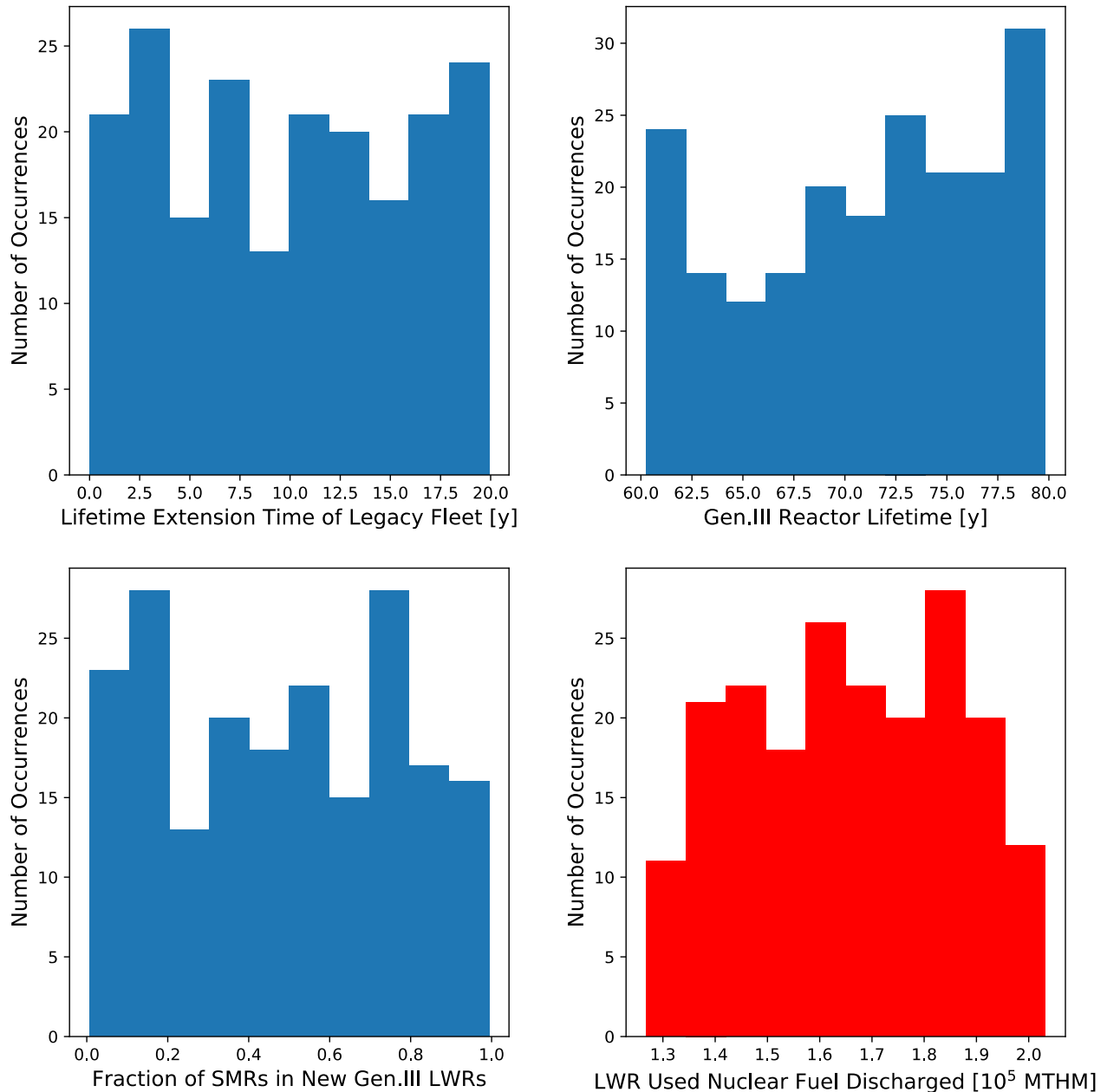

Figure 3 Histogram of the parameters are shown in blue, and the histogram of the metric is shown in red.

Table 2 Uncertainty quantification study results statistics from 200 samples

Statistics	LWR UNF discharged[TiHM]
Mean	165,445
Standard deviation	20,043
Median	165,643
Minimum	126,771
Maximum	203,192

3.1.2   Sensitivity Analysis (Single Parameter / Single Metric)

To demonstrate Cyclus/MOT's capabilities for a simple sensitivity analysis, sensitivity analyses were performed on the same 3 parameters described in Section 3.1.1. We perturbed one variable at a time, and the other two variables were kept constant at their midpoint values (10y legacy reactor lifetime, 70y Gen. III LWR lifetime, and 0.5 SMR fraction). Figure 4 shows the histograms of the parameters and metrics for this study. The histograms of the parameters are a flat block because they were sampled in a uniformly spaced grid as opposed to using a random sampling approach that produced the histograms in Figure 3 for the previous study. This sampling approach was adopted to ensure even sampling of the range to build the parametric curves/functions. The last histogram in the figure shows the distribution of the metric from each parameter sensitivity study, organized by color for each parameter; the color of the parameter histogram and metric histogram are the same.

The change in the parameter Gen-III lifetime did not cause any change in the metric, mainly because the total number of reactors deployed was constant. For the fraction of SMRs parameter, we saw a clear positive relationship, ranging from a minimum of 131,412 MTHM to a maximum of 198,485 MTHM (Figure 5). As expected, deploying more SMRs to meet power demand increases the amount of LWR UNF discharged.

For the legacy reactor lifetime extension, the relationship was more interesting (Figure 6). The eventual increase in the LWR UNF generated is due to the legacy reactors being modeled as less 'efficient' than the Gen-III fleet that consist of 50% AP1000s and 50% SMRs (*i.e.*, the legacy reactors consume more fuel per energy generated or have lower average fuel discharge burnup compared to the Gen-III fleet). So extending the lifetime of these legacy reactors will increase the LWR UNF discharged. However, note that there is a small decrease for lifetime extensions less than 8 years. This is because there is a secondary relationship/effect for this particular parameter: extending the legacy reactor lifetime will also reduce the total number of new reactors deployed in the simulation time period. The first cores of new reactors are not loaded entirely with fuel that are all at the equilibrium fissile content; there are lower fissile contents in different regions of the first core to flatten the power peaking and thus, result in fuel discharge burnups lower than the equilibrium values shown in the tables. This results in first cores producing more discharged UNF per energy generated. However, it was shown in these scenarios that this effect is only valid for extensions up to ≈8 years (*i.e.*, increasing the legacy reactor lifetimes for more than 8 years does not lead to additional reduction in reactors deployed). Thus, there are two conflicting effects with the increase of legacy reactor lifetime. Note that setting lifetime extensions to 6 years will result in the minimal value of discharged LWR UNF.

To help visualize these two competing effects, Figure 7 shows the time series evolution of LWR UNF discharged for different legacy reactor lifetime extension values. The line colors denote the discharged fuel

accumulation trend of the scenario with the corresponding legacy reactor lifetime extension. Note that the zero lifetime extension case is in red. Cases with longer legacy LWR lifetime extension (yellow) have lower mass of discharged fuel earlier in the simulation, since fewer new reactors are deployed. But later in the simulation, the longer-extension cases have more discharged fuel because the legacy LWRs are less efficient than the Gen-III LWRs. Increase in the legacy LWR lifetimes initially decreases LWR UNF discharge amount, since it decreases the total number of new reactor deployment (*i.e.*, the second wave of new Gen-III reactors built during the small window from year 2090 to 2100). Again, the UOX waste amount later increases because legacy LWRs consume more fuel per energy than Gen-III LWRs at their equilibrium operation.

This simplified study is an example of how incorporating parametric sensitivity analyses can help reveal non-intuitive effects that may be competing with one another on metric performance. In addition, although this scenario is relatively simple, it shows the potential for how this campaign can now inform on policies/decisions such as lifetime extension time with a specific number that can minimize an undesirable metric.
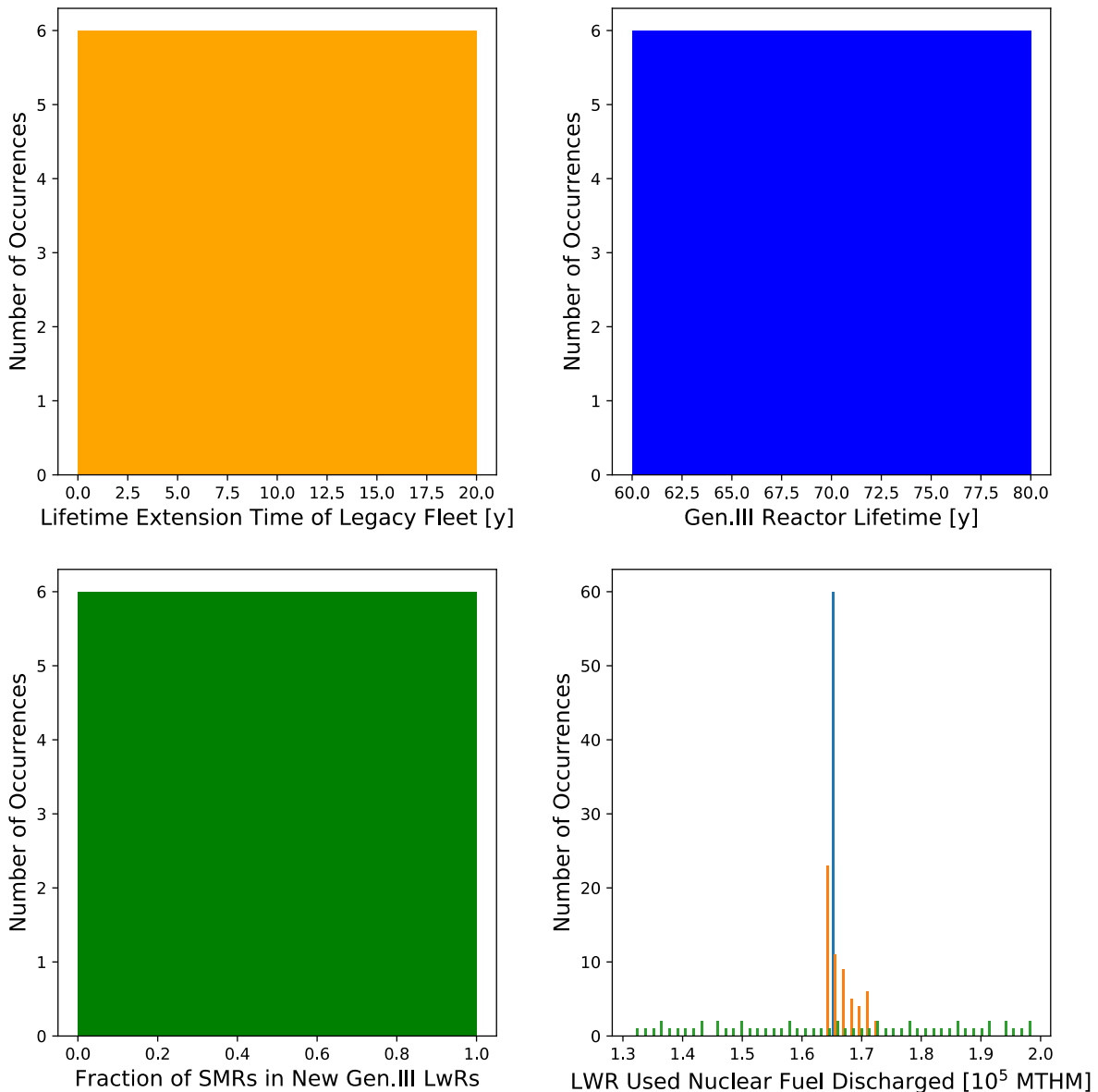
Figure 4 Histogram (sample space) of the 3 parameters and 1 metric for the single parameter sensitivity analysis
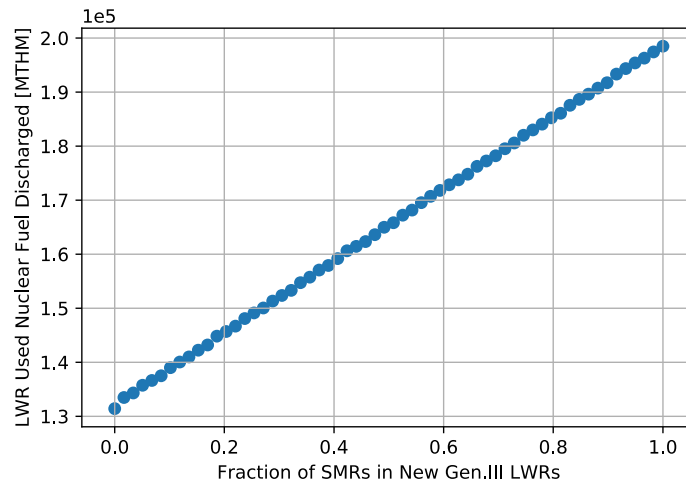
Figure 5 Relationship between Fraction of SMRs parameter and LWR UNF discharged metric
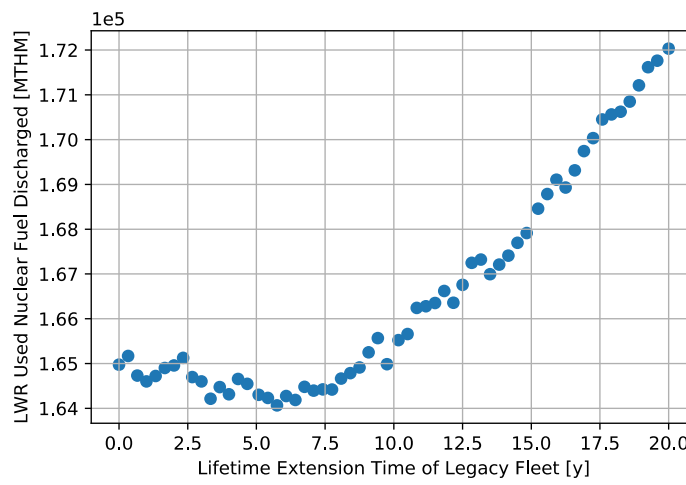
Figure 6 Relationship between LWR lifetime extension parameter and LWR UNF discharged metric
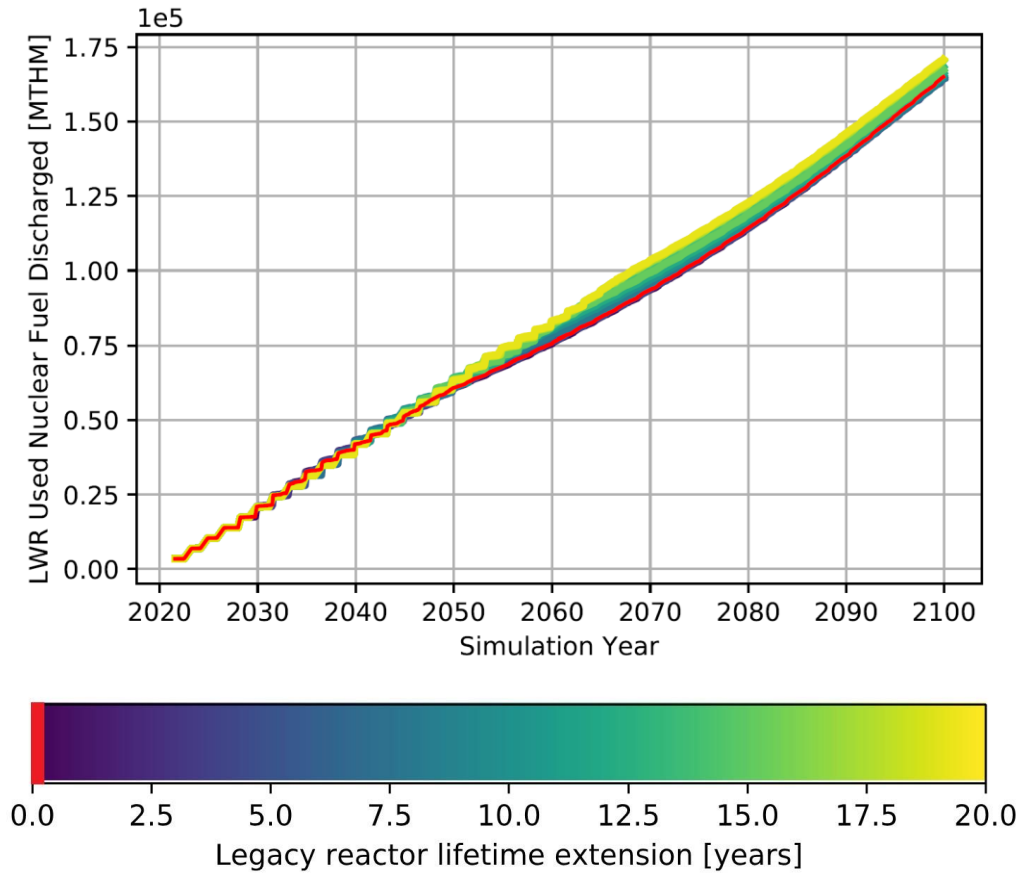
Figure 7 Time series evolution of LWR UNF discharged for different legacy reactor lifetime extension values
(the red line indicates a lifetime extension of zero)

3.1.3   Optimization (Multi-Parameter / Multi-Metric)

Having demonstrated the uncertainty quantification and sensitivity analysis capabilities of the Cyclus/MOT approach, the next study was to demonstrate MOT's optimization capabilities. Specifically, we tested the multi-objective, multivariate optimization capabilities in the MOT package by using the same 3 parameters and their parameter ranges from Scenario 1. In addition to the LWR UNF discharged metric, a second metric, number of reactors deployed, was also added with the objectives to minimize both. The optimization algorithm was run with 10 particles per generation (first generation is randomly sampled like in Section 3.1.1) and 20 generations. The hyperparameters are determined from the range and sensitivity of simulation. The optimal solution was easily found for this problem, but for problems with a wider range and higher sensitivity, they would generally require more generations and population per generation. Figure 8 shows the evolution of variables and metrics, each of the 10 particles has a different symbol or shape so it is easy to correlate the outliers shown in the metrics evolution (red) with those from the parameters (green).
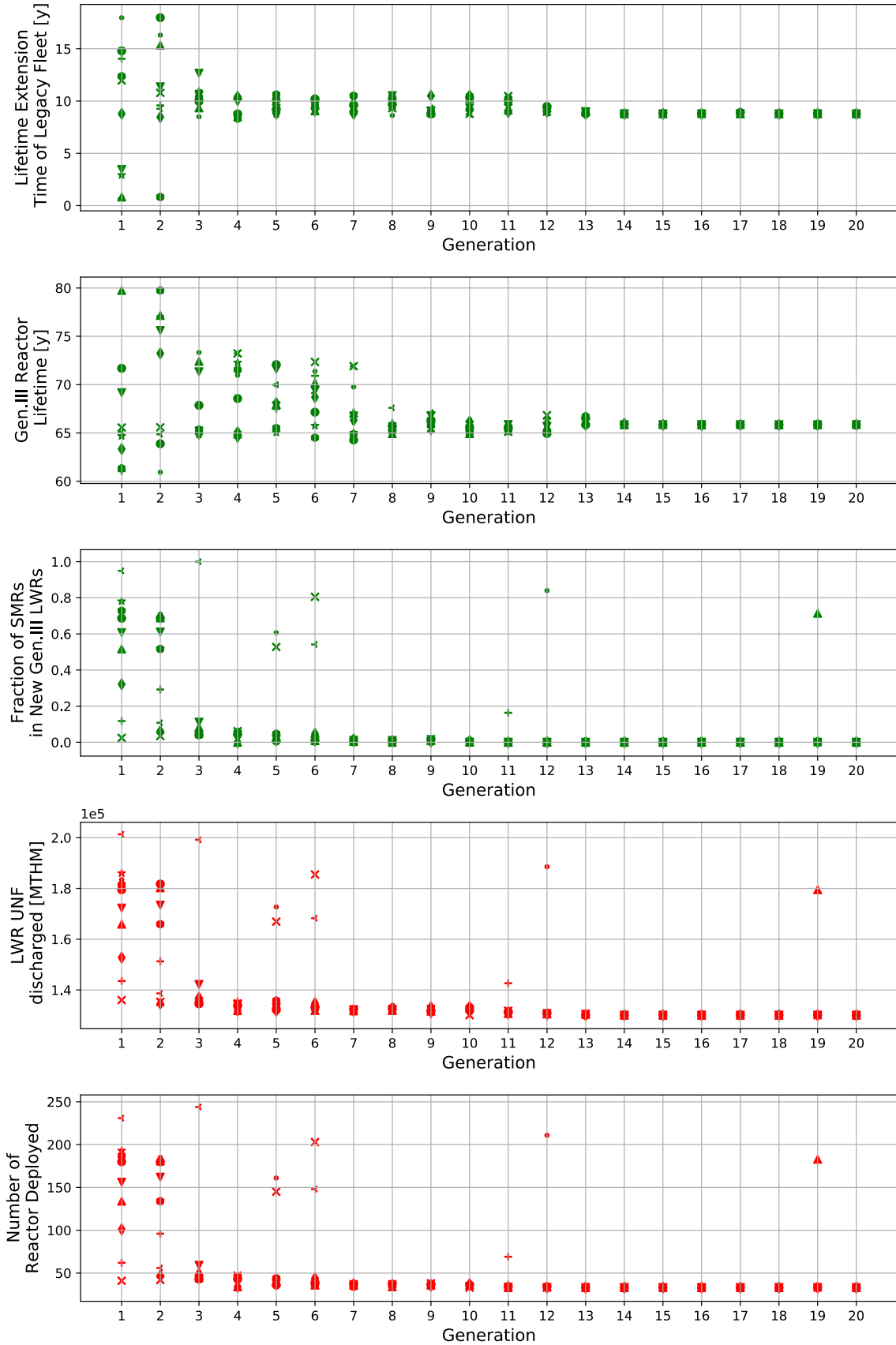
Figure 8 Evolution of parameters (green plots) and evolution of metrics (red plots) by generation.

There is a clear convergence to the optimal parameter set that yields the lowest discharged LWR UNF mass and number of reactors deployed. Recall that the program "learns" from the results of previous generations and then chooses parameters in the next generation to converge to the desired optimal results. Note that the optimum solution was obtained for the specific metrics (objective functions) used for a hypothetical scenario to demonstrate Cyclus/MOT capabilities. Thus, as shown in the next section, the optimum solution could be different when adding or changing metrics and parameters (variables) such as minimization of system cost, reprocessing capacity, etc. After a random initialization, the parameters evolve to values that yield optimum metrics. In this very specific scenario, they are 9 years of lifetime extension, 66 years of Gen. III reactor lifetime, and zero SMRs in the Gen. III LWR fleet (only AP1000s). Note that the previous optimum lifetime extension value of 6 years from Section 0 was calculated assuming a mean value for all other parameters (70 years for Gen. III reactor lifetime and 0.5 for SMR fraction). Since the algorithm is searching for the optimal set of all three parameters for the optimal metric points, the optimal lifetime extension is different from the result from the sensitivity study.

3.2   Scenario 2: Optimization of Reprocessing Capacity under Parametric Uncertainty

Now that uncertainty quantification, sensitivity analysis, and optimization were demonstrated individually using the Cyclus/MOT approach, Scenario 2 essentially combines all three into one calculation. This study examines the capability to optimize a parameter under uncertainty of other parameters. A common goal for fuel cycle simulations is to assess future demands. However, the parameters that lead to demand are uncertain, which makes it difficult to set up an optimization problem. Here, an optimization study was performed for reprocessing demand, under the parametric uncertainty of legacy LWR lifetime extension and fraction of ABR contribution to energy demand, to minimize cumulative surplus plutonium residence time and fuel shortages. In other words:

- Minimize metrics:

    - Cumulative surplus plutonium residence time [$kg \cdot$ Month]
    - ABR fuel shortages [Months]

- By optimizing parameter:

    - Reprocessing capacity [$\frac{MTHM}{month}$]

- Under the uncertainty of parameters:

    - Legacy LWR lifetime extension [0 - 20 years]
    - ABR fraction [10 - 15 % of future nuclear energy demand]

3.2.1   Scenario Description

The scenario is the same as Scenario 1 with a few exceptions: 1) the simulation is set up so that the amount of LWR UNF is not the limiting factor (*i.e.*, fuel supply to ABR is only affected by reprocessing capacity), 2) the new Gen-III reactor lifetimes are set as 80 years, 3) reprocessing begins in 2035, 5 years prior to the deployment of the first ABR, to provide enough time for the preparation of separated plutonium. Similar to Scenario 1, the depleted ABR fuel is not reprocessed, but only the UNF from LWRs is reprocessed.

3.2.2   Methodology

For depletion and fuel fabrication, the recipe method was used. An ABR fuel contains 22.1% separated transuranics (TRU) from LWR UNF, and LWR UNF has ≈ 1.04% TRU. A single batch of ABR fuel is 4,011.3 kg (886.49 kg TRU) with four batches per core. For a single ABR startup core, approximately (due to decay during cooling) 341,301.8 kg of LWR UNF has to be reprocessed (see Equations 1-3):

$$\frac{ABR \; core \; fuel \; TRU \; demand}{TRU \; fraction \; in \; UNF * \epsilon_{sep}} = \frac{LWR \; UNF \; reprocessed}{ABR \; Core} \tag{1}$$

$$\frac{\frac{kg}{batch} * batches * \frac{TRU}{fuel}}{\frac{TRU}{LWR \; UNF} * 0.999} = \frac{LWR \; UNF \; reprocessed}{ABR \; core} \tag{2}$$

$$\frac{4011.3 * 4 * 0.221}{0.0104 * 0.999} = 341{,}301.8 \frac{kg \; LWR \; UNF}{ABR \; Core} \tag{3}$$

The optimization is done using a grid search method (brute force). The entire parameter space - parameters including legacy LWR lifetime extension, ABR ratio, and reprocessing capacity - is divided up to 10 grids (Table 3) or 10 lumped values that were sampled uniformly (like in Section 0), and a sample (simulation) is generated for every combination of parameter value, which yields 1,000 samples (simulations). The simulation is run on all the generated samples, and the mean metric is examined for each reprocessing capacity value. In other words, a cross section of the 3D parametric space is taken and the 2D space is aggregated, to evaluate each optimization metric (reprocessing capacity) with a metric value. The optimization metric with the most optimal metrics is chosen as the final answer.

Table 3 Parameter grid search values

Parameter	Min	Max	Units
Legacy LWR lifetime extension	0	20	Years
ABR fraction	10	15	% power demand
Reprocessing Capacity	50,000	250,000	Kg UNF/month

3.2.3   Results

Figure 9 and Figure 10 show the correlation between each parameter and the first and second metrics, respectively, in the form of pairplots. A pairplot plots sample points as a function of two variables to visualize correlations, if it exists. The following insights can be obtained from the pairplots:

1. As expected, the reprocessing capacity parameter is positively correlated with the surplus plutonium metric (Figure 10, right graph). In other words, the more reprocessing capacity, the more surplus plutonium.

2. As expected, reprocessing capacity parameter is negatively correlated with the fuel shortage months metric (Figure 9, right graph).

3. Given the competing effects of insights 1 and 2, it was found that the optimal reprocessing capacity is between 205,555 and 227,777 kg UNF/Month. The answer is in a range rather than exact value because of the uniform sampling of lumped values (grid search), *i.e.,* we don't know the exact minimum but know that it is between these two sampled points.

4. As expected, a higher ABR fraction leads to higher average fuel shortage months (Figure 9, center graph).

5. Legacy lifetime extension of 13.3 years causes the highest average fuel shortage months (Figure 9, left graph).

   • Thus, legacy lifetime extension of 13.3 years, and an ABR ratio of 15% (the maximum fraction sampled) is the scenario that requires the highest reprocessing demand (based on insights 3 and 4).

The highest average fuel shortage occurs in the legacy lifetime extension of 13.3 years because the ABRs are deployed more aggressively during the earlier years of the second wave of rapid reactor replacements, since the new Gen-III reactors are not deployed due to the lifetime extension of legacy LWRs.
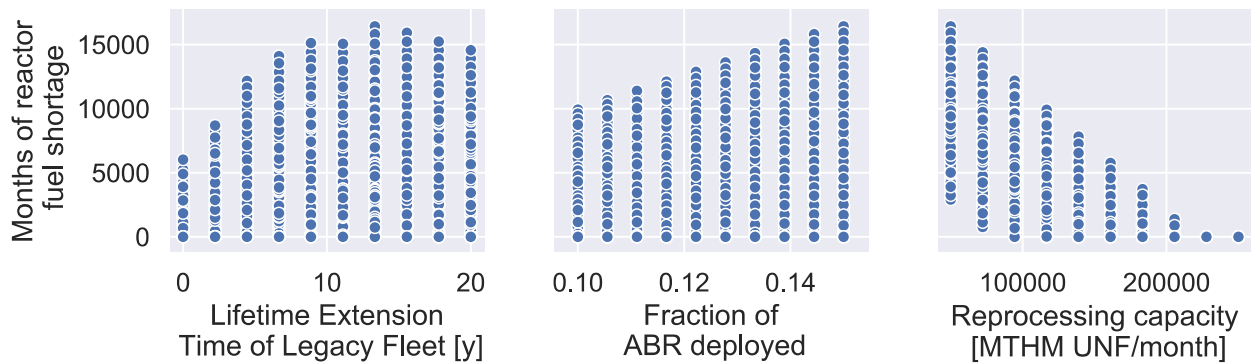
Figure 9 Pairplot of parameters (x axis) and the metric of months of reactor fuel shortage (y axis). Since the parameters are sampled discretely, the points are along the y axis.
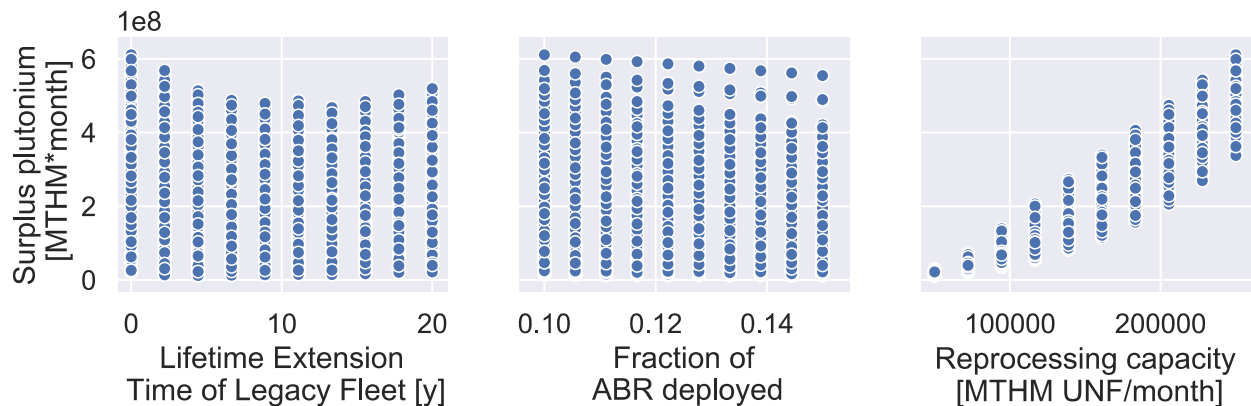
Figure 10 Pairplot of parameters (x axis) and the metric surplus plutonium inventory metric (y axis). Since the parameters are sampled discretely, the points are along the y axis.

Since the optimization parameter is reprocessing capacity, a cross section of the 3D parameter space is made for each reprocessing capacity value and is visualized in histograms to help explain the optimal parameter found (Figure 11 and Figure 12). These histograms show in detail how each reprocessing capacity value performs, by showing the distribution of the metrics it yielded, given the range of uncertain parameters (100 samples for each reprocessing capacity value). Each color denotes a reprocessing capacity value, and the histograms show the distribution of surplus plutonium values obtained from each sample generated. Note that there are no fuel shortage histograms for reprocessing capacities higher than 227,777 kg UNF/Month, meaning that no fuel shortages occur with reprocessing capacities higher than 227,777 kg UNF/month.
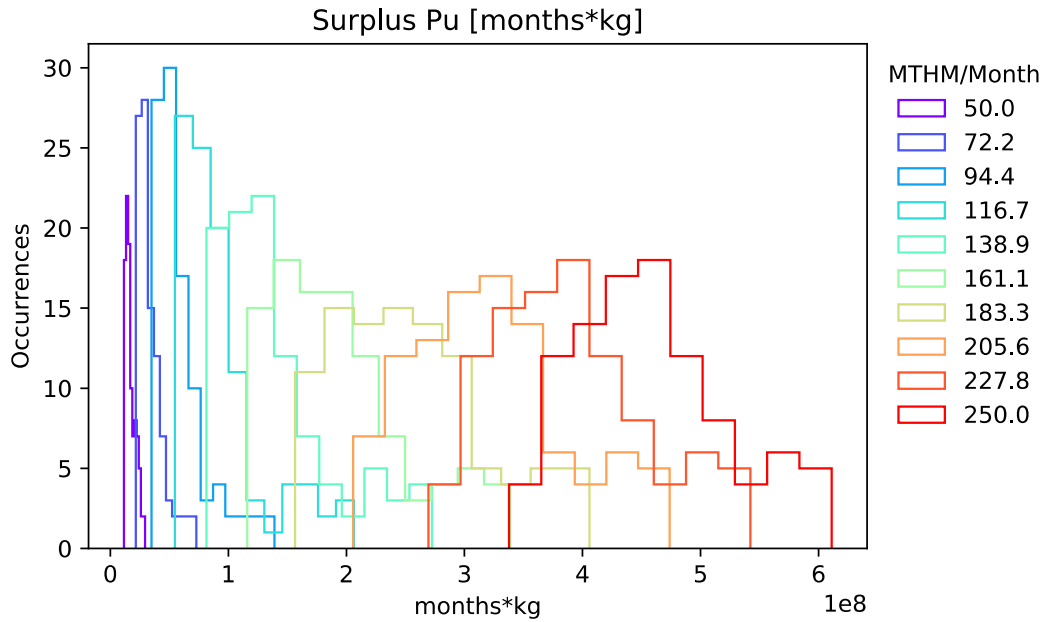
Figure 11 Histogram of surplus plutonium inventory history for each reprocessing capacity.
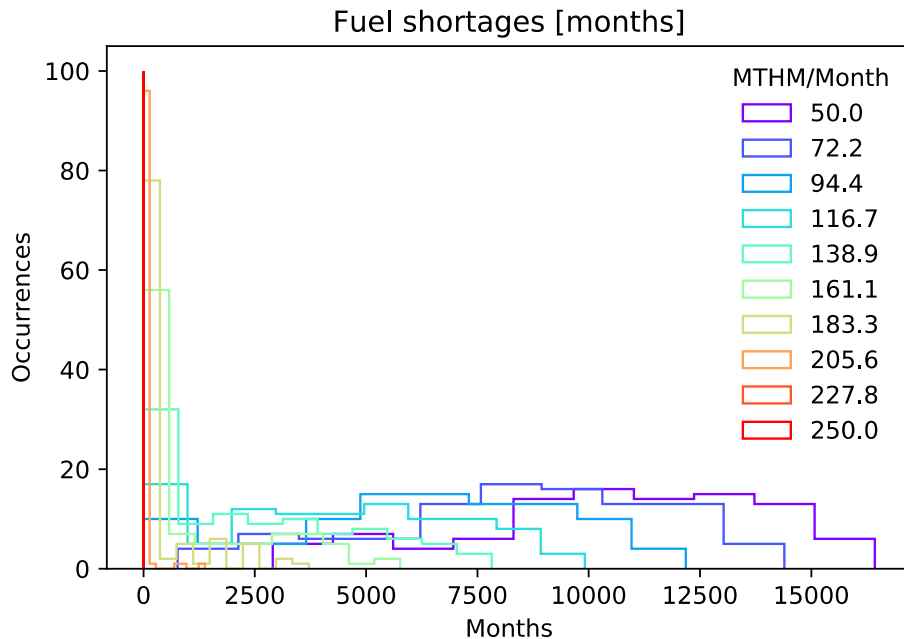
Figure 12 Histogram of ABR fuel shortage months for each reprocessing capacity.

3.3   Scenario 3: Uncertainty Quantification with Depletion

The Cyclus/MOT calculations applied to Scenarios 1 and 2 are good examples of how SA&UQ can be incorporated with NFCS results to provide much more useful information than those from standalone NFCS calculations. However, these two scenarios only involved using the recipe approach for determining fuel compositions loaded into and discharged from reactors. More complex scenarios that involve multi-recycling will require on-the-fly depletion calculations to determine fuel compositions. Thus, a third scenario was created to show the possibility of applying MOT's uncertainty quantification to depletion calculations in the Cyclus/MOT approach.

Scenario 3 is a non-transition scenario that consists of the existing fleet, consisting of 99 reactors that are identical with identical fuel compositions at charge and discharged. These reactors are gradually decommissioned from 2020 to 2050 (see Figure 13). The goal of this study is to determine the impact of a small uncertainty / perturbation of the fuel burnup on various metrics related to the back-end of the fuel cycle: total Pu inventory, total fissile Pu (Pu-239 and Pu-241) inventory, total activity of the UNF, specific activity, total decay heat of the UNF, and specific decay heat.
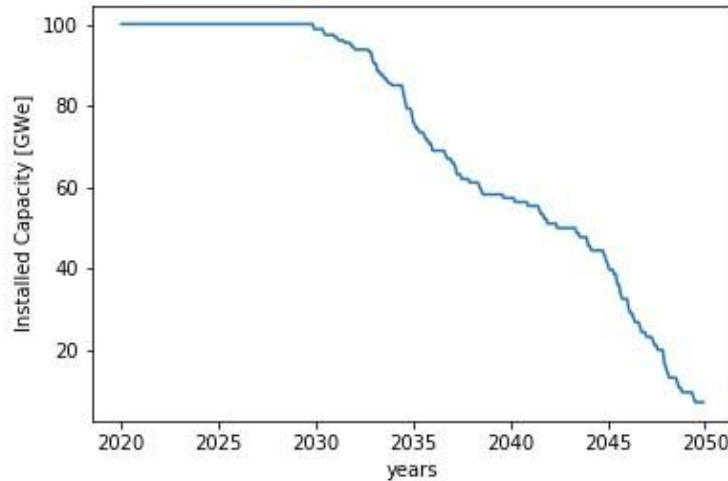
Figure 13 Nuclear capacity profile for Scenario 3.

To do this, a depletion capability was added to the MOT package by coupling Cyclus with the latest ORIGEN (*a.k.a.* ORIGEN-S). In this section, we examine the structural uncertainty of a fuel cycle simulation, namely how valid is the intentional approximation that we model all LWR UNF as having the same burnup. We do this by running explicit burnup calculations for the LWR fuel with a given perturbation in the burnup (5% in this study). We developed a module (archetype) within Cyclus that couples SCALE/Oak Ridge Isotope GENeration (ORIGEN) with Cyclus to perform in-simulation depletion calculations. The module uses an f33 file (*i.e.*, ORIGEN library file with transmutation matrix data), which was generated from an external SCALE transport calculation. During the Cyclus run, the module reads the f33 file, creates an ORIGEN input file to perform appropriate depletion calculations, runs ORIGEN, and reads back the depleted calculations. This new capability allows the users to define assembly-wise burnup values (*i.e.*, for each assembly for each batch), or have the module calculate the batch-wise burnup from its operating parameters via Eq. 4:

$$BU_{calc} = \frac{P_{elec} * \frac{1}{\epsilon_{th \to elec}} * T_{cycle} * N_{batch}}{M_{core}} = \frac{MWth * d}{MTHM} \qquad (4)$$

A 5% random perturbation (Eq. 5) was introduced to model uncertainty in discharge burnup data. Essentially, we are assigning a 5% parametric uncertainty to the depletion model used in these calculations to see the impacts on the back-end fuel cycle characteristics due to the structural approximation of constant burnup.

$$BU = BU_{calc} \cdot (1 + Unif(-0.05, 0.05)) \tag{5}$$

$$BU = Burnup$$

$$Unif(-0.05, 0.05) = \text{Sample from uniform distribution from} -0.05 \text{ to } 0.05$$

With the random perturbation built into the reactor module, the entire scenario is run 200 times.

3.3.1   Results

Each simulation took 7.5 minutes on a laptop (8GB RAM, Intel i9 processor, 8 cores). Table 4 show that a random perturbation up to 5% of the discharge burnup of reactors does not cause a significant variation (≤ 1%) in any of the metrics. These metrics were calculated by ORIGEN for each run. The variation is represented by the statistic coefficient of variation (Eq. 6).

$$Coefficient\ of\ Variation = \frac{Std.dev}{Mean} * 100 \tag{6}$$

Fissile plutonium fraction denotes the fraction of Pu-239 and Pu-241 in the plutonium inventory. Figure 14 shows histograms of the total and fissile Pu inventories in the entire UNF inventory, and Figure 15 shows histograms of the activity, specific activity, decay heat, and specific decay heat. The activity and decay heat are calculated at discharge.

Table 4 Statistics of metrics (calculated at discharge) for Scenario 3

Metric	Units	Mean	Std. deviation	Coeff. Variation
Pu inventory	kg	4.247E+05	1.272E+03	0.299
Fissile Pu inventory	kg	2.950E+05	1.066E+03	0.362
Decay heat	MW	4.808E-01	3.177E-03	0.661
Activity	Bq	4.666E+29	2.791E+27	0.598
Specific decay heat	MW/kg	8.732E-09	5.770E-11	0.661
Specific activity	Bq/kg	8.473E+21	5.068E+19	0.598
Fissile Pu fraction	-	6.944E-01	1.244E-03	0.179

Figure 14 Histogram of plutonium inventories.
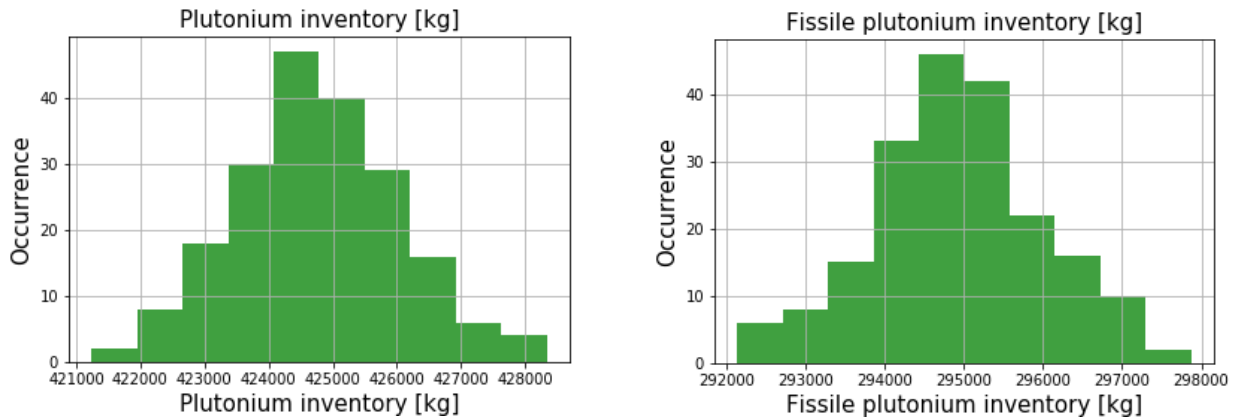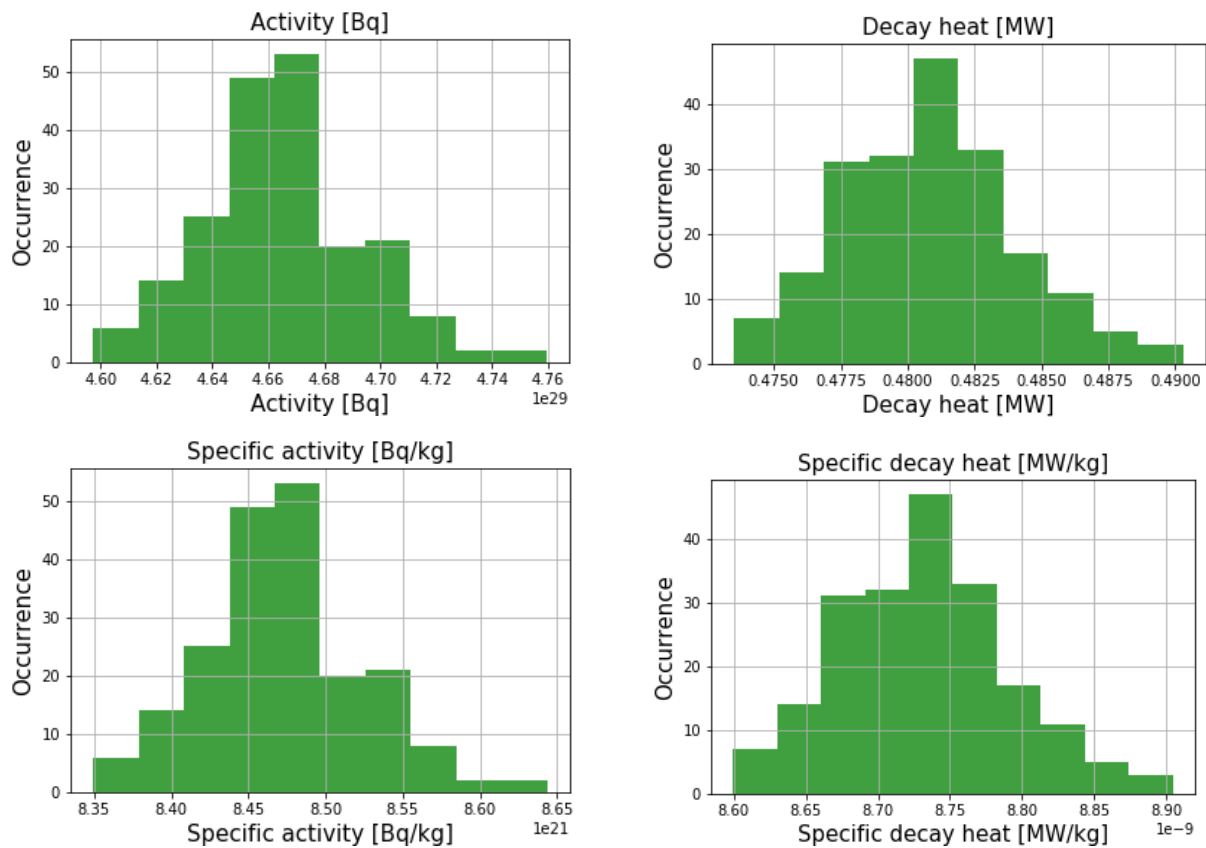

Figure 15 Histogram of decay heat and activity of the UNF inventory.

3.3.2   Conclusions

Although the scenario and parameters selected here did not produce a major physical takeaway, a series of simple exercises demonstrated the capability to perform uncertainty quantification in Cyclus/MOT on the structural uncertainty of an explicit isotopic depletion capability.

4.   DYMOND/Dakota Results

DYMOND allows for accurate representation of the dynamic changes in nuclear fuel compositions through its coupling with ORIGEN (currently, ORIGEN-2) for depletion calculations and direct critical fuel composition calculations. The analysis framework allows us to leverage this reduction in model structural uncertainty to better understand the parametric uncertainty. For the initial investigation of the NFCS SA&UQ capabilities, the parameters were chosen based on experience of the limiting factors in the transition from the current U.S. once-through nuclear fuel cycle to a closed cycle with reprocessing. The response metrics were chosen to be in line with several of the evaluation criteria chosen for the U.S. Nuclear Fuel Cycle Evaluation and Screening Report [Wigeland *et al.,* 2014]. Three different SA&UQ studies were conducted, each demonstrating unique features of the DYMOND/Dakota tool: Assessment of the Failure Space, Sobol' Indices, and Analysis of Variance (ANOVA).

4.1   Scenario Description: Fuel Cycle Transition to SMRs and FRs

The fuel cycle transition scenario that is the basis of the study is a transition from the current U.S. nuclear fuel cycle to a fuel cycle consisting of small modular light water reactors (SMRs) and advanced fast reactors (FRs) designed to operate in an actinide burning, rather than breeding, regime. Since the SMRs are LWRs that operate in once-through mode with LEU, it is still technically part of the initial fuel cycle, hence this can be considered a "partial" transition. Note that the advanced fast reactor performance parameters were obtained from a gas-cooled fast reactor (GFR), which was selected purely for academic reasons. Given the many fuel cycle simulations from this Campaign involving the SFR technology, it was desirable to assess the fuel cycle performance of a fast reactor technology with continuous recycle other than the SFR for this first example application of the DYMOND/Dakota capabilities.

This partial transition is set to begin in 2020 with spent fuel being stored for reprocessing starting in 2020, reprocessing beginning in 2035, advanced reactors first being deployed in 2040, and the simulation terminating in 2100. The scenario begins with the current U.S. nuclear fleet consisting of legacy pressurized water reactors (PWR) and boiling water reactors (BWR) where each is modeled using the average power, capacity factor, fuel enrichment, fuel batch reload mass, effective full power days per cycles, number of in-core cycles per batch, final burnup, and thermodynamic efficiency of reactors of currently operating of the same type (Table 5). These reactors are also modeled to have the average operational lifetime of 60 years with reactor start dates being back-calculated such that shutdowns are in-line with currently announced plans for shutdown or approved license extensions as of February, 2020 [NRC 2020].

Deployment of currently announced and under construction reactor projects (AP-1000s Vogtle reactor 3 and 4 planned for start-up in 2021 and 2022 as well as NuScale-UAMPs SMR installation planned for start-up in 2027) were also included and modeled as Gen-III PWRs with design and operating specifications matching those reported for the NuScale SMR [Ingersoll *et al.,* 2014]; the much larger AP-1000 reactors were approximated as an installment of 4 of these reactors. These Gen-III SMRs are deployed to meet projected nuclear energy demand (Figure 16) until advanced reactors can begin to be deployed in 2040. The advanced fast reactors are based on a modified design of the GFR-2400 [Stauff *et al.,* 2015] where the fuel stream has been allowed to have a greater concentration of transuranics, and the operation of the reactor reaches a higher average final burnup by extending the cycle length. The deployment of the advanced fast reactors is designed as a gradual market intrusion, linearly increasing to meet a 40% share of new-build reactor-capacity, calculated on a 5-year moving average, at the end of the simulation in 2100.

The deployment schedule for all reactors after 2027 (the last year that a new reactor is currently planned to startup) is calculated to meet the projected nuclear energy demand [Kim 2020], following the guidelines of which reactors are able to be deployed, with the smallest excess of additional capacity possible. The caveat to those guidelines, though, is that the first FR is required to be started in 2040 regardless of demand, and

that all reactors must operate at their listed capacity factor for the entirety of their operating lifetime (*i.e.*, no load following or extended shutdowns unless there is a fuel shortage). This results in overproduction of energy in 2048-2051 (see Figure 17), equivalent to multiple SMRs' capacities due to a predicted sharp decline in demand that greatly exceeds the rate of loss of capacity from reactors shutting down. However, outside of these years, the deployment schedule closely matches the demand, with excess capacities of less than one SMR-equivalent, while also closely following a linear increase in advanced reactor deployment rate. At the end of the simulation this ramping of advanced reactor deployment culminates in FRs being 31.2% of nuclear energy generating capacity (Figure 16).

Table 5 Design and operational specifications for all reactors modeled in the study

	PWR	BWR	SMR	FR
Reactor power (MWe)	1007	1044.375	300	1100
Capacity factor	0.92	0.93375	0.92	0.89
Thermal efficiency	0.34945	0.339687	0.3125	0.5
Equilibrium burnup (GWd/MTHM)	50	45	37.3	49.8
Number of batches	3	3	3	3
Cycle length (EFPD)	493	682	672	481
Operational lifetime	60	60	60	60
Annual Fuel Requirement (MTHM/yr)	19.3533	23.2857	8.6426	14.3508
Core Load (MTHM)	85.2398	139.7882	51.8863	63.7470
Average Batch Enrichment (U-235/U)	4.54%	4.18%	4.54%	N/A

While the LWRs in the study are refueled using enriched uranium oxide fuel, the advanced reactors in the study are fueled primarily from reprocessed fuel streams from all reactors, including FRs, containing uranium, plutonium, and all other minor actinides. No enrichment of this reprocessed material is performed, instead the fuel composition is found using the DYMOND criticality search functionality. This calculates a fabrication ratio of reprocessed material to a make-up material (in the case of this study either depleted uranium from the enrichment process or natural uranium which is considered sufficiently plentiful) for each fuel batch requested by a reactor. The reprocessed material streams are differentiated by their reactor of origin, and the material stream used for fuel fabrication is dictated by the defined source priority of the reactor requesting the fuel. The FR design in the study prioritizes fuel sources in the order of SMR, legacy PWR, legacy BWR, and finally FR with unlimited recycle. This priority was chosen based on the reactivity worth of the reprocessed spent fuel from each of the source reactors, prioritizing the material stream that required the minimal actinide content to achieve end-of-cycle criticality. The available material for advanced reactor fuel fabrication can be seen in Figure 18, which shows that there is no significant stock of material from SMRs (all were used) and the stocks of legacy reactor reprocessed materials are fully depleted by 2070 and 2078 for the PWR and BWR origin material, respectively. The stock of reprocessed FR material reaches a maximum of 289.67 tonnes in 2084. This is also the date with the greatest total amount of reprocessed material in storage (292.79 tonnes).
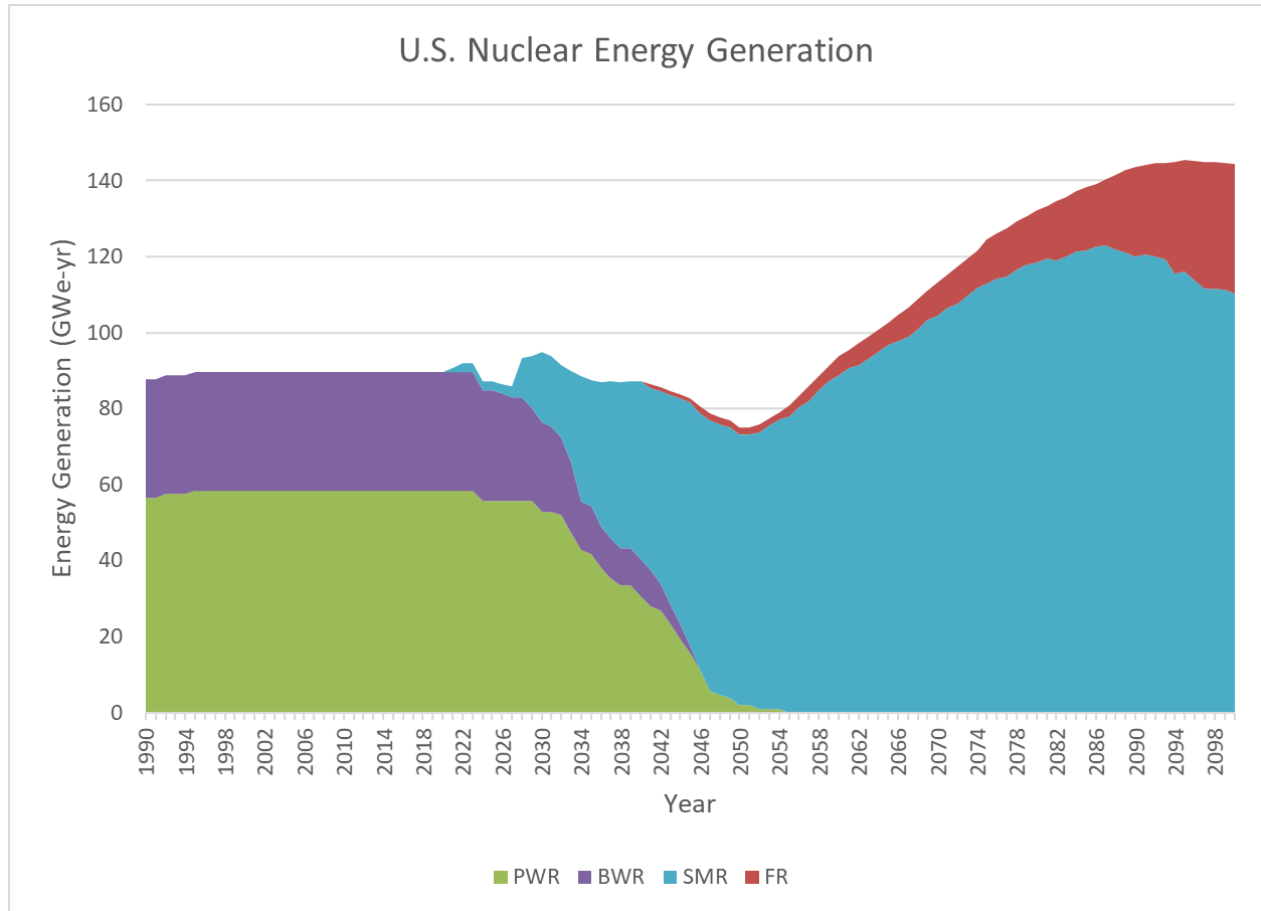
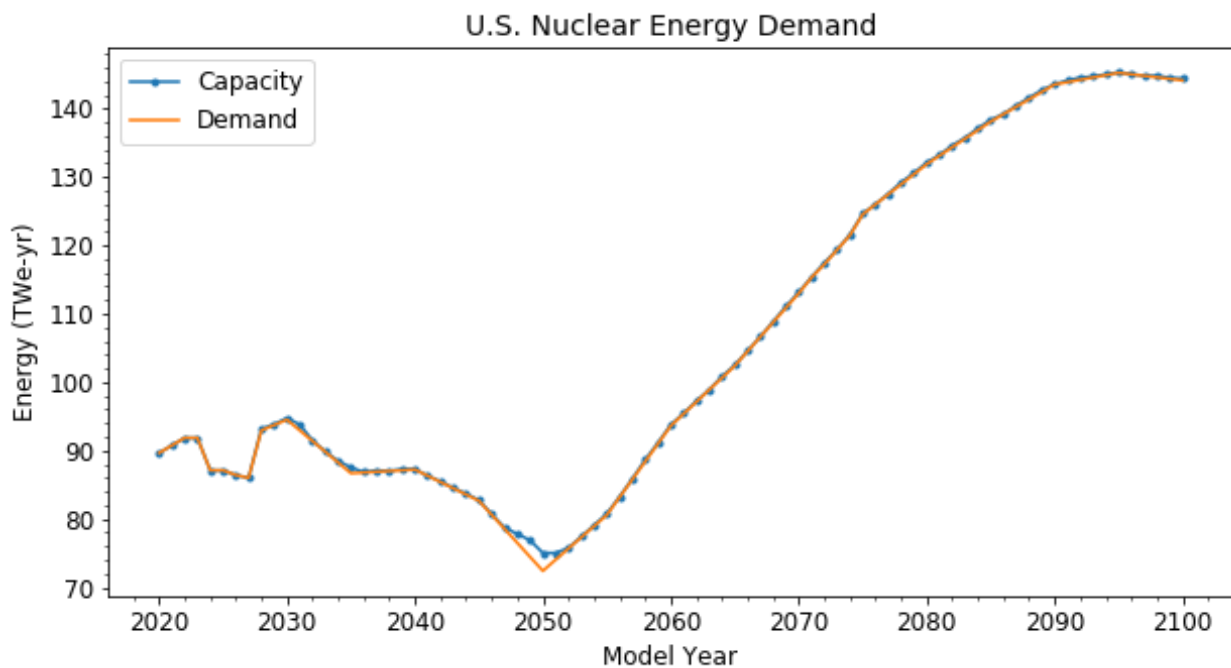Figure 16 Base scenario energy production by reactor type

Figure 17 Base scenario U.S. nuclear energy demand and total generating capacity
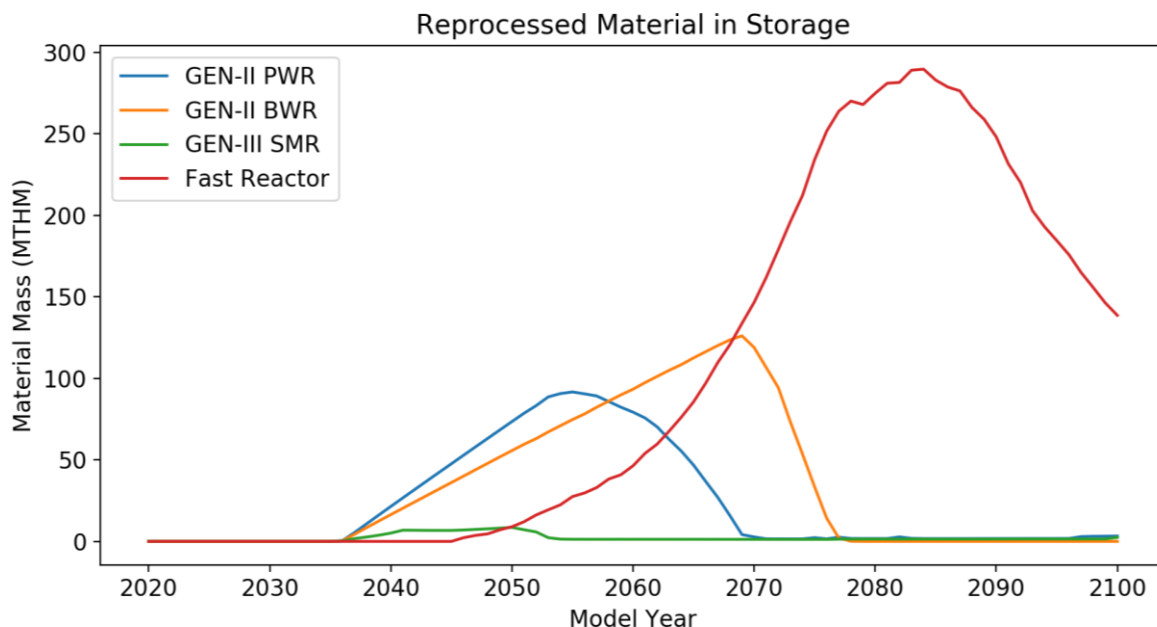
Figure 18 Reprocessed material available for use in FR fuel fabrication by reactor of material origin

The reprocessing facilities for this study are modeled as bulk processes where only one facility of each type exists and the plant capacity is the capacity for the entirety of the fuel cycle. There are two type of reprocessing types modeled – an aqueous process based on Purex facilities but with no separation of uranium or plutonium from the minor actinides, and a pyroprocessing process. Both types are modeled to be batch process (*i.e.*, no mixing or distribution of residency times) with 0.1% losses and a process time of 1 year. However, the aqueous reprocessing requires the used fuel to be cooled for 5 years post discharge and the pyroprocessing only requires 2 years of cooling before reprocessing. The two methods of reprocessing are used to account for the different characteristics and operational knowledge in reprocessing of the used fuel streams. Aqueous reprocessing is used for the LWR used fuel due to the existing facilities using aqueous reprocessing methods and the demonstrated high capacity of these facilities to reprocess LWR fuel. Pyroprocessing was chosen for the FR used fuel stream due to the higher flexibility of the process to allow for various fuel forms, higher temperatures of the fuel, and fabrication of radioactive fuel.

In the preliminary work to develop the base scenario, the capacity of the aqueous reprocessing was the main determinant of whether there was a fuel shortage and the pyroprocessing capacity determined the peak mass of reprocessed material in storage. This is due to the priorities given to the fuel streams. The reprocessing of the LWR fuel must be high enough to keep up with the fuel requirements for the deployment of the FRs, with startup cores requiring the most total mass. The reprocessing of the FR fuel must build up a sufficient stockpile so that once the Gen-II LWRs' fuel has been used there is enough to support the new reactor deployment until the end of the simulation. The minimum capacities then are correlated, as a lower capacity to reprocess the LWR fuel results in less being available for starting up FRs early in the simulation, so a higher reprocessing capacity for the FR fuel is required to meet demand. However, this would also result in the stock of LWR fuel from prior to the start of the first FR lasting longer. The minimum combined capacity, with no fuel shortages, if reprocessing begins in 2035 is found to be approximately 1000 MTHM/year. For the base scenario to be more representative of an "average" scenario, rather than one on the periphery of the parameter space for the study, the total capacity was set at 1,500 MTHM/year. This capacity was divided amongst the two types of reprocessing as 1,200 MTHM/year for the aqueous process and 300 MTHM/year for the pyroprocessing.

4.1.1   Study Parameters

Four variables of the fuel cycle transition were chosen as the parameters for this study –

1. **The start date of the reprocessing facilities (RPS)**: This parameter controls the year that both reprocessing facilities would begin operation and ranged between the beginning of the simulation (2020) and the startup date of the first advanced reactor (2040). Given that range restriction of this variable made the difference in startup date of pyroprocessing inconsequential, as all dates are prior to any FR used fuel being ready for reprocessing, both facilities are modeled as having the same startup date. In sampling of this parameter only integer values were allowed, as that is the modeling restriction placed on the variable by DYMOND, but when using surrogate models for the calculation, RPS is considered continuous.

2. **The annual reprocessing capacity (RPC) for the reprocessing facilities:** This parameter controls annual capacity for each of the reprocessing types, where both types are given the same capacity. The decision to set the capacities to be equal was made for three main reasons. The first is to reduce the number of independent variables considered in the study. The second is that in the preliminary work to develop the base scenario, it was found that the capacity for the pyroprocessing facility did not significantly impact the overall transition behavior unless the capacity of the aqueous reprocessing facility was low enough to be comparable. Finally, because the pyroprocessing plant is available at the start of operation of the advanced reactors, the true rate of reprocessing will either be limited by the rate of used advanced reactor fuel being generated or the reprocessing capacity will be so small as to be insignificant compared to the total reprocessing capacity and fuel production for the advanced reactors, effectively reducing the fuel cycle studied to be a single-recycle system rather than unlimited-recycle. This parameter ranges between 500 MTHM/yr/facility and 3000 MTHM/yr/facility, putting the entirety of the study safely in the regime of the used advanced reactor fuel production rate being the limiting factor.

3. **A scaling factor for the year-to-year growth of nuclear energy demand (GSF):** This parameter scales the energy demand increase, or decrease, between years based on the change in the base case scenario. However, the demand prior to 2027 does not change, as those years are considered constant and set by current data rather projections. The range of GSF is from 0 to 4, where any factor less than 1 would be a decrease in the demand growth rate and a factor of 0 would be a constant demand.

4. **The advanced fast reactor share of new-build reactor-capacity at the end of the simulation (NBS):** This parameter not only effects the build rate of advanced fast reactors at the end of the simulation but also the build rate of advanced fast reactors for the duration of the transition as the new build share of advanced fast reactors is calculated to scale linearly from the first deployment in 2040 up to the NBS in 2100. This parameter has a large effect on every part of the fuel cycle, as every additional FR that is deployed reduces the number of SMRs deployed by approximately 3. This increases the usage of reprocessed material in fuel fabrication, while also significantly decreasing the supply as less SMR used fuel is required per tonne of fabricated FR fuel than FR used fuel. This parameter ranged from a 10% final share (0.1) to 50% (0.5). If this range were chosen as anything less than 10%, it would result in very few FRs being constructed, and thus being too similar to the current U.S. fuel cycle, and a share of greater than 50% would result in too many scenarios having fuel shortages.

The sampling of these parameters was ensured to be evenly distributed across the ranges through the Dakota LHS and OAS sampling methods, as can be seen in the distribution of sampling points in Figure 19. The sampling of 2400 scenarios was uniformly distributed for all parameters with the lower quartile, median, and upper quartile values equally dividing the range between the extreme values. The results of this sampling was used in the training of the surrogate models, with the number of samples chosen

based on the guidance in the Dakota user's manual. The suggested minimum number of samples for variance decomposition studies (such as Sobol' indices and ANOVA) is:

$$100 * P * (R + 2)$$

Where *P* is the number of parameters being sampled and *R* is the number of response being generated from the parameter set. This minimum is to ensure sufficient coverage of the parameter space and a high statistical significance of response variance. In the reduced parameter space sampling this same number of samples is used, however, when using the surrogate models the number of samples is increased to 10,000 as the computational cost for increasing the number of samples is insignificant – on the order of seconds of computational time.
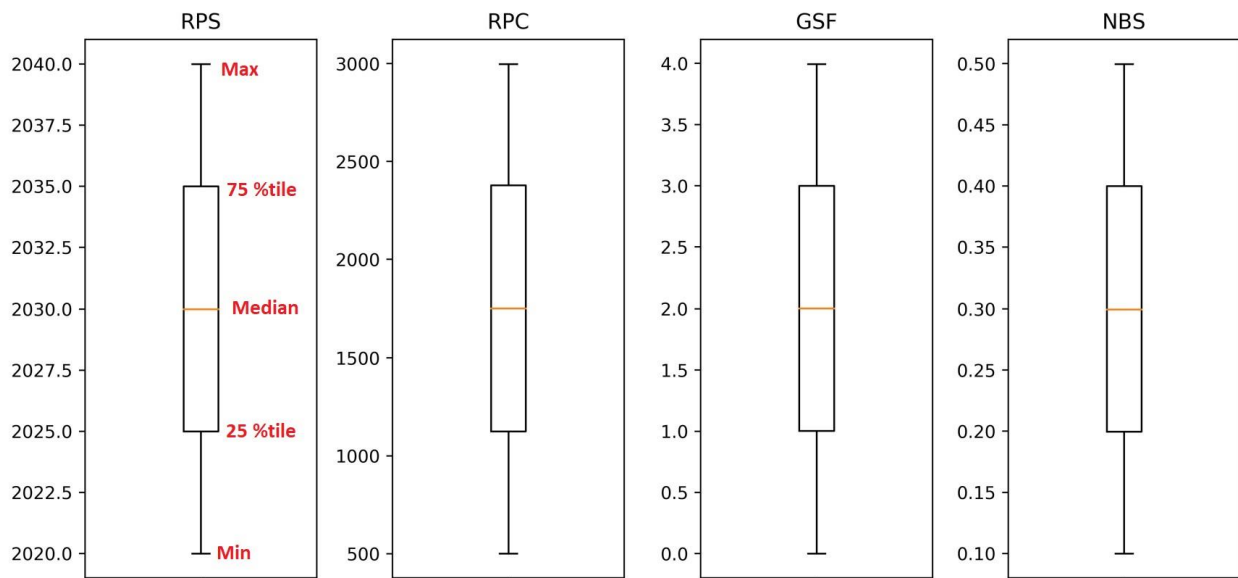
Figure 19 Box plots of the samples

4.1.2   Response Evaluation

The purpose of the study is to quantify the sensitivity of four response metrics — total mass of natural uranium consumed in (MTU/GWe-yr), maximum annual enrichment capacity required (Tonne SWU/GWe-yr), mass of nuclear waste that requires disposal (MTHM/GWe-yr), and the levelized (in 2020 US$/GWe-yr) cost of the fuel cycle transition with component costs estimated based on the Advanced Fuel Cycle Cost Basis Report [DOE 2017]. These four response metrics were chosen to closely resemble several of the criteria used in the U.S. Nuclear Fuel Cycle Evaluation and Screening Report [Wigeland *et al.*, 2014]. The four response metrics were calculated from values in DYMONDs output – a database record of annual stocks, flows, compositions, and state points at critical points in the fuel cycle – and normalized to the total energy produced in the scenario.

The calculations for each metric is explained below:

1. Total mass of natural uranium consumed (NatU) – This response is calculated as the difference in the stock of natural uranium at the beginning of the simulation and the end of the simulation divided by the summation of energy produced in each year. This method is used, as opposed to tracking all outflows of natural uranium to the enrichment facility and as make-up material in fuel fabrication, because DYMOND does not consider mining activities and as such there is no material stream that can increase the initial stock of natural uranium.

2. Maximum annual enrichment capacity required (T-SWU) – DYMOND does not explicitly place a limit on the annual reprocessing capacity in the model, it is instead set *a priori* to be whatever is required to meet the enrichment needs of the fuel fabrication for that given year. Therefore the Tonne-SWU enrichment capacity is calculated from the material flows and compositions of the natural uranium, depleted uranium, and enriched uranium through the enrichment facility by:

$$W_{SWU} = P * V(x_p) + T * V(x_T) - F * V(x_F)$$

$$where, \quad V(x) = 1 - 2x * \ln\left(\frac{1-x}{x}\right)$$

In these equations P is the mass of enriched uranium produced, T is the mass of depleted uranium produced, F is the mass of natural uranium required to produce masses P and T, and x is the respective enrichments of the material corresponding to the subscript. This value is tracked for each reactor independently at each year in a scenario, with the response using the maximum annual total across all reactors.

3. Total mass of nuclear waste that requires disposal (Disp) – All materials in the simulation that are not being stored as a stock for another potential use (*e.g.*, used fuel that will be reprocessed, depleted uranium that can be used as make-up material in fuel fabrication, *etc.*) will be directed to final disposal and are considered nuclear waste. However, DYMOND tracks all sources and material streams separately. In other words, each reactor type will have two contributing material streams – spent fuel directly from the reactor, and high-level waste that is from the reprocessing facility with that reactor-type of origin. This allows for waste streams to be differentiated, but in the case of this response metric all materials are assumed to be equal. This assumption allows for the total mass disposed to be calculated as the difference in mass in disposal at the start of the simulation and at the end of the simulation, with the addition of the mass of material that is "waiting for disposal" due to cooling time restrictions.

4. Levelized cost of the nuclear fuel cycle during transition (Cost) – The calculation of the levelized cost of the transition is the most complicated, accounting for 20 separate factors in the fuel cycle. The factors are listed in Table 6 are taken from table S-1 in 2017 cost basis report [DOE 2017]. These factors are detailed as, and used with, the following assumptions:

- Natural Uranium Mining and Milling (module A1) - The cost of extracting uranium ore and purifying it based on historical data of uranium "yellow cake" commodity prices.

- Conversion Process (module B) - The cost of further purification of the U_3O_8 and conversion to UF_6 in solid cylinders for feed to an enrichment plant based on 2017 market values.

- Enrichment (module C1) - The cost of enriching UF_6 from natural enrichment of 0.711% to a product value in the range of 3-5% and tails in the range 0.25-0.35% based on 2017 market value of all production of LEU and cost of raw uranium to enrichment operating cost.

- Virgin LEU UO_2 Fuel Fabrication (module D1-1) - The average cost of fabricating the many current LWR fuel forms from freshly enriched LEU with Zircaloy cladding including all related costs including materials and inspections.

- Remote handled fuel fabrication from reprocessed material (module D2/F2) - The cost of fabricating fuel from highly radioactive reprocessed material extrapolated from small scale production facilities and pilot plant production.

- COEX Total Aqueous reprocessing of UOX fuel (module F1) - The cost of used fuel reprocessing from cask reception to product and byproduct stream stabilization and storage. The costs are

based on the 2006 Areva facility estimates, with the COEX process being chosen due to the product stream being the closest match to that desired for the FR design.

- Electrochemical and remote handling fuel recycle (module F2/D2) - The cost of fuel reprocessing using pyro-processing through the same steps as the aqueous reprocessing. The cost is based on studies that were available at the time of the evaluation and extrapolated costs based on the difference in the e-chem process and the UREX process.

- Co-located storage of reprocessed transuranic fuel material (module E3-1b) - The cost of safe, indefinite, short-term storage of mixed transuranic actinide products derived from thermal and/or fast reactors extrapolated from costs of current facilities in the US and internationally.

- Thermal LWR Costs (module R1) - Construction and O&M costs for light water reactors based on historical data of construction and operation in U.S., including gen 3+ construction plans and estimates available at the time of the report.

- Fast Reactor Costs (module R2) - Construction and O&M costs estimated based on experience with sodium fast reactor extrapolated to N^{th} of a kind scale deployment of large reactors.

- Aqueous reprocessing derived HLW conditioning, storage, and packaging (module G1-1A) - The cost to receive, stabilize, and store high level waste in preparation for final disposal in accordance with NRC, DOE, and EPA regulations. This disposal assumes no significant concentration of TRU. The costs are calculated based on the reprocessing plants at La Hague and Sellafield.

- Electrochemical reprocessing derived HLW conditioning, storage, and packaging (module G1-2A) - The costs to receive, stabilize, and store high level waste derived from electrochemical reprocessing by vitrification. The costs were developed as part of the CFTC Follow-on EAS.

- Spent fuel conditioning and packaging (module G2) - The cost to transfer spent fuel to a final storage cask from either wet or dry onsite storage and transfer the spent fuel to its future site. The costs are based on 2017 costs for casks and spent fuel conditioning for dry storage.

- Geological Repository for spent fuel (module L1) - The final disposal costs as calculated by the Yucca Mountain Project and its successor the DOE-NE Used Fuel Campaign.

- Geological Repository for HLW (module L1) - The final disposal costs as calculated by the Yucca Mountain Project and its successor the DOE-NE Used Fuel Campaign.

The costs in Table 9 are being applied to either direct values from the DYMOND model, or values that have to be derived from other values due to the construction and material management of the model. These values, how they are represented in the output, and how costs are applied to them are described going from the head end of the fuel cycle through to final disposal, and all output masses are in units of tonnes:

- The mining, milling, and conversion costs are all applied at the same time and are calculated based on the sum of the natural uranium, enriched uranium, and enrichment tails flows. This value is in the output labeled as "Mined ore".

- The enrichment costs are relative to the annual required kg-SWU. This is calculated in the DYMOND model for all reactor types separately and is output as "SWU required".

- The fuel fabrication costs are calculated for all LWRs together (PWR, BWR, and SMR) and the FR independently. The FR is assumed to be the Nth reactor type in the implementation and all other types are assumed to be LWRs. This assumption is also true for all other costs that are unique to reactor type such as reprocessing, HLW storage, and construction and operating costs. The

reprocessing costs are assessed upon the material entering the reprocessing facility and is in the output as "SNF reprocessed".

- The cost of construction is assessed at the end of the first year that the NPP is operational is scaled based on plant capacity. A new NPP coming on line is described as "New Capacity" in the output as opposed to the "Installed capacity" of reactors that were already operational.

- O&M costs are assessed at the end of the year and scaled by the amount of power that the NPP produced during that year. The reactors power for the year is output as "Produced electricity" and is given in units MWe. This power is scaled to account for capacity factor, and unless there is a fuel shortage, is therefore accounting for refueling outages.

- The cost of SNF storage is assessed at the time that the fuel goes to the reprocessing facility or is sent to interim storage. The amount that enters these storages is not directly modeled in DYMOND but are instead calculated as the change in the stock of spent fuel at the two location plus the amount that was removed. For the fuel at the reprocessing facility the values in the output of the stock are labeled as "Spent fuel waiting for RP", and the output flows is equal to what is going into the reprocessing plants. The storage facility inventory is labeled in the output as "Spent fuel in storage" and the flow leaving storage is "Spent fuel readying for disposal". Both of these are assessed the same storage costs.

- The HLW going into storage is directly modeled in DYMOND and is labeled in the output as "HLW to storage".

- The disposal costs of the spent fuel and the high level waste are both calculated directly as those amounts of each being disposed are given in the output as "Spent fuel being disposed" and "HLW being disposed" respectively. Both of these values are treated as a gross sum with no origin or age distinction being made.

Table 6 Fuel cycle costs from table S-1 in 2017 cost basis report [DOE 2017]

Component	units	2017$	2020$
Nat U mining/milling	$/kgU	86	89.44
Conversion	$/kgU	13	13.52
Enrichment	$/kg-SWU	125	130
Fuel Fab- PWR UO$_2$	$/kgHM	400	416
Fuel Fab- BWR UO$_2$	$/kgHM	400	416
Fuel Fab- RH Fuel Fab	$/kgHM	1400	1456
Reprocessing – Oxide	$/kgHM	1562	1624.48
Reprocessing - Electrochemical RH	$/kgHM	1200	1248
TRU Storage	$/kgTRU	950	988
LWR Construction	$/KWe	4400	4576
LWR O&M fixed component	$/KWe-yr	73	75.92
LWR O&M variable component	$/KWh	0.0018	0.001872
FR Construction	$/KWe	4100	4264
FR O&M fixed component	$/KWe-yr	76	79.04
FR O&M variable component	$/KWh	0.0022	0.002288
Storage Aqueous HLW	$/kg	5700	5928
Storage E-chem HLW	$/kg	17214	17902.56
Storage SNF	$/kgHM	135	140.4
Repository SNF	$/kgHM	600	624
Repository HLW	$/kgFP	6000	6240

4.1.3   Fuel Cycle Transition "Failure" Determination

In the study, a fuel cycle transition scenario is considered to have failed if at any point in the simulation an insufficient amount of energy is generated to meet the demand. With the generation capacity of the fleet and reactor deployments strictly calculated to exceed the demand, this failure state can only be reached if an otherwise operational reactor is not generating power. In the current DYMOND model, this state can only be reached through a fuel shortage. Furthermore, the state can only be reached by a shortage in the primary fuel fabrication material feed from reprocessed used nuclear fuel due to enrichment capacity at any given time step being equal to the required capacity to meet demand. This then means that fuel shortages, and therefore scenario failures, are only the result of reactors that are defined to take fuel fabricated from reprocessed material and no other source. The advanced reactors in this study meet that definition.

A scenario failure is defined as such so that it not skew the sensitivity analysis results. Since all response quantities are power specific, the decreased generation during a fuel shortage could lead to adverse effects that over-emphasize, or are counter to, the local sensitivity of those parameters. Also, in the case that the results of a sensitivity analysis study are used for optimization, or to inform decisions, these failures could lead to undesired outcomes such as the quantity of material going to final disposal being minimized through reactor shutdowns due to fuel shortages.

In global sensitivity analysis, failures result in meaningless solutions. This is due to both the Sobol' indices and ANOVA calculations relying on matching sets of samples with identical parameter values in one dimension to be able to measure the influence of the other parameters independent of that dimension. Three methods for removing failures were demonstrated in this study:

1) Limiting the parametric space of the study: Assuming that the failures are constrained to the extreme values of one or more of the parameters, as is the case for this study, this solution will provide an accurate global measure of the sensitivity of the reduced region without introducing any new assumptions or biases. However, if in the removed parameter space, there were successful scenarios they will no longer have influence over the results as potential solutions.

2 & 3) Quadratic regression model and Gaussian process model: As mentioned in Section 2.2.2, the other solution for the issue of failed scenarios is the creation, and sampling, of surrogate models for determining global sensitivity measures. Dakota offers many surrogate modeling methods including polynomial regression, Gaussian process, and machine learning. In this study a quadratic regression model and Gaussian process model are created from the successful transition scenarios from the 2400 samples of full parameter space described in Section 4.1.1. Calculating sensitivities from these surrogate models precludes the potential of failures while being able to sample the full range of potential parameter values. However, this also introduces a bias by being able to sample regions in the parameter space that do not meet the requirements of the transition scenario.

4.2   Simulation Results

To demonstrate the capabilities of DYMOND/Dakota, three different SA&UQ studies were conducted: Assessment of the Failure Space, Sobol' Indices, and Analysis of Variance (ANOVA).

4.2.1   "Failure" Space

In deterministic models the ranges of parameter values, or combinations of parameter values, that can result in a "failure" will define a region referred to as a "failure" space. In the case of this study, the parameters that most control whether a transition scenario will have a fuel shortage, and therefore be counted as a failure, are the reprocessing start date (RPS), the reprocessing capacity (RPC), and the share of new builds that are FR advanced reactors (NBS). RPC and NBS have a strong synergistic effect on fuel shortages, as a function of those two parameters defines one edge of the failure space. It is likely, given the results of the

sensitivity analysis, the energy demand growth (GSF) also has a synergistic affect with NSB and RPC to cause fuel shortages. However, either this effect is secondary to that of RPC and NBS, or the sampling region of the study does not contain that edge of the failure space.

RPS defines a hard cut-off – a single parameter defined edge of the failure space – for successful transitions. As can be seen in Figure 20, fuel shortages occur as early as 2020 when the reprocessing starts with small capacity, but disappear with sufficient reprocessing plant capacity. However, regardless of reprocessing plant capacity, starting reprocessing any time after 2038 results in fuel shortages. This is from the characteristics of the reprocessing plants and fuel fabrication process – both have a process time of 1 year. If the first reprocessing plant begins operation in 2039, regardless of its capacity, no fuel can be ready for the first FR to startup at the start of 2040. This relationship therefore is obvious at the reprocessing capacities studied, resulting in 202 of the 259 failed scenarios. However, if either the initial deployment of advanced reactors was higher, or if the reprocessing capacity in the fuel cycle was very low, it is expected this direct relationship would be synergistic with the other parameters. This would be a result of multiple years of accumulation of reprocessed material being needed to meet the demand of the larger startup fuel loading. In order to remove this failure pathway from the limited region sampling RPS was limited to the range of 2020-2038.
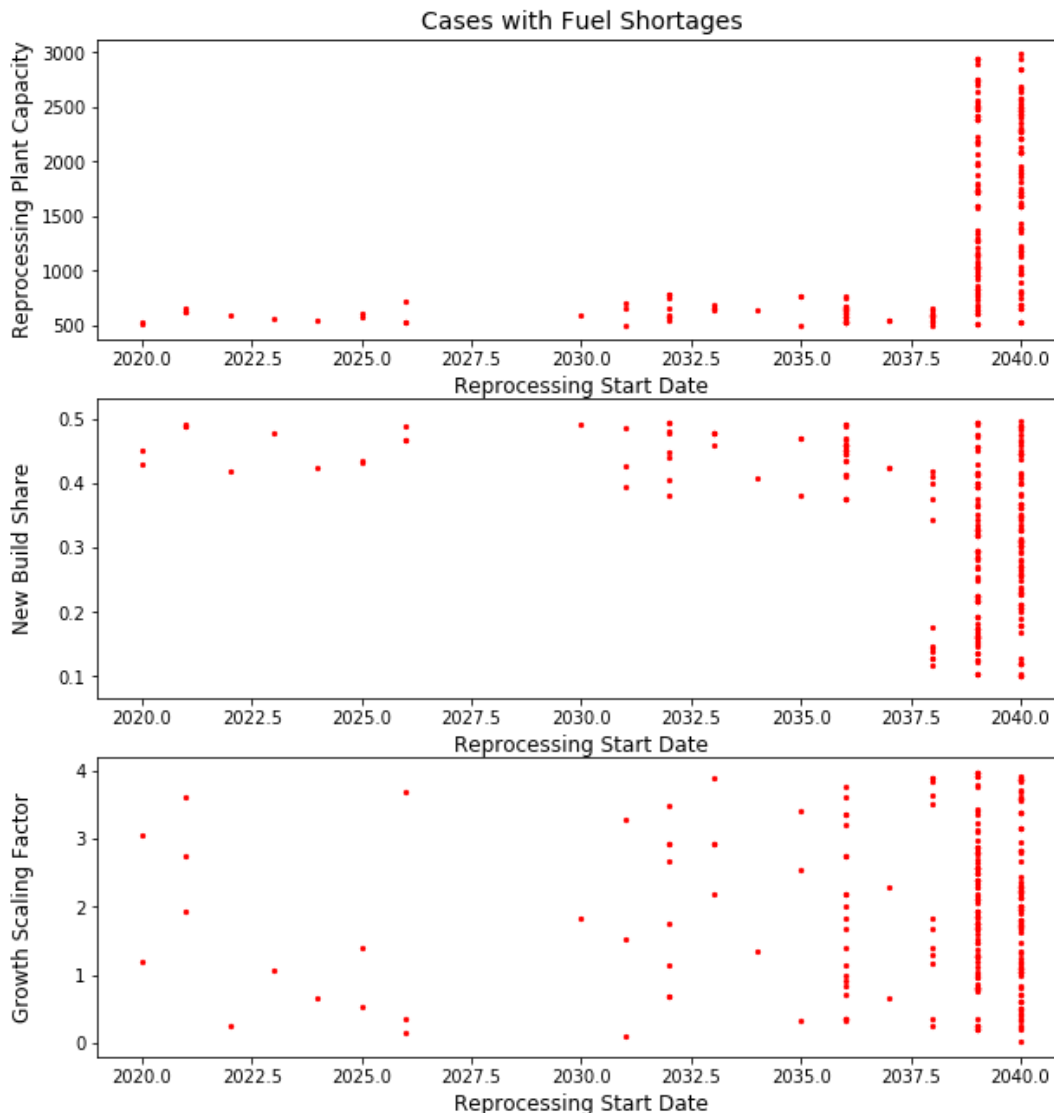

Figure 20 Parameters of scenarios that resulted in a fuel shortage

The other primary contributor to fuel shortages, responsible for the other 57 failed scenarios, is the relationship between NBS and RPC. Fuel shortages arose at some point in the transition for cases with a high NBS and a low RPC. These shortages are more difficult to predict as they come at later times in the scenario. Figure 21 illustrates how the relationship between the two parameters defines one edge of the failure space. The slight overlap of the successes and failures in the figure is due to it being a two dimensional projection and, as stated earlier, GSF has a slight influence on this failure type at this boundary point. Due to this boundary being curved it is more difficult to account for in the reduced sampling space study. Rather than trying to match the curve of the boundary, RPC was limited to the range of 785 MTHM/yr to 3000 MTHM/yr. This effectively sets the reprocessing capacity high enough that there will be sufficient material at even the highest deployment rate of FRs in the study.

Through this "Failure" space study, it was possible to determine quantitatively two decisions that needed to be made to remove all fuel shortage scenarios given the assumptions: start reprocessing between 2020 and 2038 and keep the reprocessing capacity above 785 MTHM/yr.
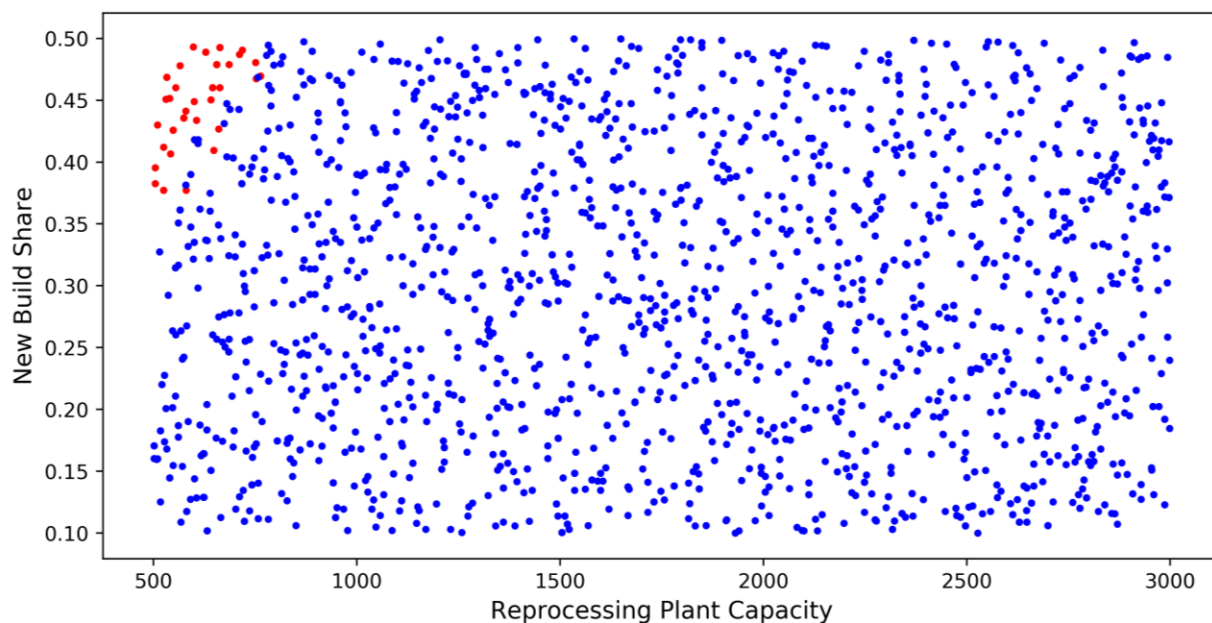

Figure 21 The sample space of reprocessing capacity for each of the two plant types and the advanced reactor new build share at the end of the simulation. (RED – fuel shortage, BLUE – successful transition)

4.2.2   Sobol' Indices

Sobol' indices give a measure of the contribution of each parameter to the variance observed in a response metric. In the case of DACE with deterministic models, the variance is the same as the range of values of the output that are possible given a range of values of the inputs, *i.e.*, the importance of a parameter to a response metric. There are two measures provided by Sobol' indices, the main effect index and the total effect index. The main effect index indicates the fraction of the variance that a parameter is solely responsible for. This is measured by the ratio of variance that is observed in the response metric at each point that the parameter is constant, averaged over all other parameters, to the total variance in the response. The total effect index is a measure fraction of the main effect of the parameter and all synergistic effects that parameter has with the other parameters. In this context, a synergistic effect may be a

constructive or destructive interaction of any order between two or more parameters that results in the behavior of the response metric not being purely additive from the main effects of the constituent parameters. The total effect is measured as the ratio of the average variance in the response, when only the parameter being measured is allowed to vary, to the total variance in the response. This measurement is akin to a quantification of the average behavior that would be observed from doing many parametric studies on the parameter being measured at different sets of values of the other parameters. These measures of importance were calculated for the three methods of removing failures, introduced in Section 4.1.3, in Table 7, Table 8, and Table 9.

While the three failure elimination methods agree on the main contributors for each response metric, the difference in magnitudes of these importances indicates that the removed range of values in the limited parameter space has a significant effect on the total variance and the distribution of the variance. This means that the limited parameter space is not exactly representative of the larger space and the effects observed are nonlinear and non-additive. In particular, the importance of the NBS doubles from the total parameter space, as measured by the surrogate models, to the limited parameter space for the cost of the transition. This would indicate that much of the impact of the demand growth scaling factor on cost comes from scenarios with low reprocessing capacities. This is also seen in the other metrics, however, those effects are not as pronounced. Due to these effects, only the indices calculated from the surrogate models will be considered measures of the global sensitivity for this study.

The four response metrics each have only one or two variance contributing parameters. Though all four parameters are given measured index values, an index of less than 0.01 is in effect statistical noise as it is two orders of magnitude smaller than the primary contributors and therefor smaller than the resolution of importance for this study. **The primary contributing parameter for three of the four response metrics** (~97% to natural uranium consumption, ~95% to enrichment capacity needed, and ~75% to mass of waste disposed) **is NBS**, which also is one the two contributors of the fourth response. The primary contributor of the fourth response metric (~76% to total cost of the transition) is the demand growth scaling factor, GSF.

Table 7 Main effect indices and Total effect indices for the limited parameter space sampling

Response Metric	Parameter	S_i -Main Effect	S_{TOT} - Total Effect
Natural Uranium Consumed	Reprocessing Capacity (RPC)	0	0
	Demand Growth (GSF)	0.041	0.019
	FR New Build Share (NBS)	0.937	0.916
	Reprocessing Start Date (RPS)	0	0
Maximum Tonne-SWU Required	Reprocessing Capacity	0	0
	Demand Growth	0.02	0.039
	FR New Build Share	0.892	0.87
	Reprocessing Start Date	0	0
Tonne Waste Disposed	Reprocessing Capacity	0.18	0.128
	Demand Growth	0.024	0.013
	FR New Build Share	0.846	0.766
	Reprocessing Start Date	-0.007	0.001
Cost of Fuel Cycle Transition	Reprocessing Capacity	0.006	0.004
	Demand Growth	0.486	0.831
	FR New Build Share	0.374	0.468
	Reprocessing Start Date	0.002	0.002

Table 8 Main effect indices and Total effect indices for the quadratic regression surrogate model

Response Metric	Parameter	Sᵢ -Main Effect	Sₜₒₜ - Total Effect
Natural Uranium Consumed	Reprocessing Capacity (RPC)	0.001	0
	Demand Growth (GSF)	0.001	0.004
	FR New Build Share (NBS)	0.972	0.974
	Reprocessing Start Date (RPS)	0	0
Maximum Tonne-SWU Required	Reprocessing Capacity	0	0
	Demand Growth	0.001	0.003
	FR New Build Share	0.972	0.975
	Reprocessing Start Date	0	0
Tonne Waste Disposed	Reprocessing Capacity	0.205	0.236
	Demand Growth	0	0.002
	FR New Build Share	0.749	0.747
	Reprocessing Start Date	0.001	0.002
Cost of Fuel Cycle	Reprocessing Capacity	0.007	0.011
	Demand Growth	0.798	0.784
	FR New Build Share	0.183	0.194
	Reprocessing Start Date	-0.001	0.002

Table 9 Main effect indices and Total effect indices for the Gaussian process surrogate model

Response Metric	Parameter	Sᵢ -Main Effect	Sₜₒₜ - Total Effect
Natural Uranium Consumed	Reprocessing Capacity (RPC)	0	0.001
	Demand Growth (GSF)	-0.001	0.006
	FR New Build Share (NBS)	0.968	0.972
	Reprocessing Start Date (RPS)	0.001	0
Maximum Tonne-SWU Required	Reprocessing Capacity	0	0.007
	Demand Growth	0.005	0.02
	FR New Build Share	0.95	0.98
	Reprocessing Start Date	0.005	0.004
Tonne Waste Disposed	Reprocessing Capacity	0.203	0.233
	Demand Growth	-0.003	0.005
	FR New Build Share	0.749	0.748
	Reprocessing Start Date	0.004	0.002
Cost of Fuel Cycle	Reprocessing Capacity	0.007	0.058
	Demand Growth	0.762	0.827
	FR New Build Share	0.157	0.247
	Reprocessing Start Date	-0.008	0.013

The share of advanced fast reactors deployed directly, and strongly, impacts the first two parameters due to the increase in advanced fast reactors eliminating the deployment of many LWRs which drive the need for natural uranium and enrichment. The effect on waste disposed is also direct in that more of the material being reprocessed in the fuel cycle originates from LWRs at low NBS, which generates more high level waste (HLW) as a byproduct of reprocessing. Reprocessing capacity is a secondary contributor to mass of waste disposed, with a positive trend indicating an increase in reprocessing capacity results in a greater quantity of waste produced, however this is a result of the model setup. After the start of stockpiling a reactor type's used fuel for reprocessing, it only contributes to waste as HLW coming from reprocessing. Due to this, for most of the scenarios with aqueous reprocessing, the limiting factor in HLW produced is the capacity of the reprocessing plant as there is always a surplus of LWR UNF waiting to be reprocessed. Similarly, the effect of NBS on the total cost of the transition is not intuitive, as the overall cost of the advanced reactors and the associated facilities are more expensive but an increase in the new build share of advanced reactors reduces the transition cost. However, due to fewer of the FRs being needed to replace SMRs, and that the cost of the reprocessing facilities and fuel fabrication facility is not directly tied to the deployment of advanced reactors, an increase in the share of advanced reactors does result in a decrease in total transition cost. These trends can be visualized in the figures in **Appendix B: Response Metrics of all Scenarios Modeled in DYMOND**, which illustrate how strongly the variance in a metric contributes to the overall variance by the spread in the data along a trend line.

The parameters and responses in this study were chosen to have predictable relationships in order to be able to judge the efficacy of the sensitivity analysis methods, and as such one or two parameters were intended to be the dominating contributors with little or no interaction in most response. However, as indicated by the total effect index for GSF for natural uranium consumption and RPC for the cost of the fuel cycle transitions, there are synergistic effects. These effects are indicated by the total effect index for the parameter being much larger than the main effect. Though which combination of factors are causing the effect can be explicitly found from the indices, it can be inferred from the relative total and main indices. In the case of natural uranium consumption, NBS is the directly-contributing parameter, and no other parameter has a meaningful total index, making the relationship easy to infer. However, for the cost response metric, there are two directly contributing factors – NBS and GSF. However, given that the total effect for both RPC and NBS are a greater fraction of the effect index than for the main effects, it can be inferred that the synergistic effect is dependent on these two parameters and not GSF. This effect is minor though, contributing approximately 5% of the total variance.

4.2.3   ANOVA Analysis

The Analysis of Variance (ANOVA) method for importance decomposition separates a parameter range into groups. In this study, Dakota creates these groups via orthogonal arrays and uses statistical tests to determine the variance in and between these groups and to determine if the variation in the response is attributable to a parameter. The tests then quantify how confident you can be that the variation is statistically significant. The default statistical test available in Dakota for testing the ANOVA hypothesis is the F-test. This test determines statistical significance by comparing the mean square within a group against the mean square between groups. The ratio of the two is referred to as the F-value (Fdata in Dakota) and follows a scaled chi-squared distribution. The F-value for no relationship between the parameter and the response (*i.e.*, the null hypothesis) is one, and as the F-value increases, the more unlikely the variance observed is uncorrelated to the variance in the parameter. The null hypothesis can therefore be rejected if there is a sufficiently small probability that an F-value greater than one can be observed happening by chance. This probability is the p-value. In general for ANOVA hypothesis testing, a confidence value would be used to determine if the p-value is small enough, however, in this study the effect of the parameters was not ambiguous, as can be seen in Table 10 with the p-values being binary.

The results obtained from the ANOVA agrees with the Sobol' indices on the primary contributing parameters for each response. However, **the advantage of using the Sobol' indices for NFCS results is that the relationships between the parameters are better defined**. Whereas, the ANOVA results do not identify any of the secondary contributors as statistically significant except that perhaps some synergistic effects can be seen by the differences in the ratio of the within group and between group sum of squares and mean sum of squares. This is due to the sampling and analysis methods. ANOVA takes a courser approach that is more compatible with traditional experimental data, with each parameter being split into 40 "treatment" groups. Variance based decomposition with Sobol' indices, though, allow for many more unique evaluation groups (several hundred for the same number of samples) and better isolation of directly contributing and synergistic factors.

Table 10 Results of Analysis of Variance Study (ANOVA)

Response Metric	Parameter	Source of Variation	Degrees of Freedom	Sum of Squares	Mean Sum of Squares	F-value	p-value
Natural Uranium Consumed	Reprocessing Capacity	Between Groups	40	5.59E-08	1.40E-09	3.67E-03	1.00E+00
		Within Groups	1640	6.25E-04	3.81E-07		
		Total	1680	6.25E-04			
	Demand Growth	Between Groups	40	2.17E-06	5.42E-08	1.43E-01	1.00E+00
		Within Groups	1640	6.23E-04	3.80E-07		
		Total	1680	6.25E-04			
	FR New Build Share	Between Groups	40	6.21E-04	1.55E-05	5.91E+03	0.00E+00
		Within Groups	1640	4.31E-06	2.63E-09		
		Total	1680	6.25E-04			
	Reprocessing Start Date	Between Groups	40	6.05E-08	1.51E-09	3.97E-03	1.00E+00
		Within Groups	1640	6.25E-04	3.81E-07		
		Total	1680	6.25E-04			
Maximum Tonne-SWU Required	Reprocessing Capacity	Between Groups	40	1.58E-10	3.96E-12	1.16E-02	1.00E+00
		Within Groups	1640	5.60E-07	3.41E-10		
		Total	1680	5.60E-07			
	Demand Growth	Between Groups	40	1.68E-09	4.21E-11	1.24E-01	1.00E+00
		Within Groups	1640	5.58E-07	3.40E-10		
		Total	1680	5.60E-07			

Response Metric	Parameter	Source of Variation	Degrees of Freedom	Sum of Squares	Mean Sum of Squares	Fdata	p-value
	FR New Build Share	Between Groups	40	5.50E-07	1.37E-08	2.22E+03	0.00E+00
		Within Groups	1640	1.02E-08	6.19E-12		
		Total	1680	5.60E-07			
	Reprocessing Start Date	Between Groups	40	2.22E-10	5.54E-12	1.62E-02	1.00E+00
		Within Groups	1640	5.60E-07	3.41E-10		
		Total	1680	5.60E-07			
Tonne Waste Disposed	Reprocessing Capacity	Between Groups	40	8.68E-09	2.17E-10	1.22E+01	0.00E+00
		Within Groups	1640	2.90E-08	1.77E-11		
		Total	1680	3.77E-08			
	Demand Growth	Between Groups	40	5.54E-11	1.38E-12	6.03E-02	1.00E+00
		Within Groups	1640	3.77E-08	2.30E-11		
		Total	1680	3.77E-08			
	FR New Build Share	Between Groups	40	2.88E-08	7.19E-10	1.32E+02	0.00E+00
		Within Groups	1640	8.95E-09	5.46E-12		
		Total	1680	3.77E-08			
	Reprocessing Start Date	Between	40	4.46E-11	1.12E-12	4.86E-02	1.00E+00
		Within	1640	3.77E-08	2.30E-11		
		Total	1680	3.77E-08			
Cost of Fuel Cycle Transition	Reprocessing Capacity	Between Groups	40	9.13E+06	2.28E+05	3.84E-01	1.00E+00
		Within Groups	1640	9.75E+08	5.95E+05		
		Total	1680	9.84E+08			
	Demand Growth	Between Groups	40	7.38E+08	1.85E+07	1.23E+02	0.00E+00
		Within Groups	1640	2.46E+08	1.50E+05		
		Total	1680	9.84E+08			
	FR New Build Share	Between Groups	40	1.87E+08	4.67E+06	9.59E+00	0.00E+00
		Within Groups	1640	7.98E+08	4.86E+05		
		Total	1680	9.84E+08			

		Between Groups	40	2.17E+06	5.43E+04	9.07E-02	1.00E+00
Reprocessing Start Date		Within Groups	1640	9.82E+08	5.99E+05		
		Total	1680	1680	9.84E+08		

5.   Conclusions

This year, two approaches for coupling the SA&I Campaign's nuclear fuel cycle simulators with SA&UQ tools were successfully executed, and the powerful new features were demonstrated on simple to complex scenarios of nuclear fuel cycle transition. Specifically, the Cyclus/MOT approach was used to demonstrate applications to fuel cycle uncertainty quantification, sensitivity analysis, and optimization for single and multiple parameter and metric considerations. For these example scenarios, the problem was set such that there is a single optimal point, but that rarely is the case for most engineering problems. For a more robust testing of the multi-objective - multivariate optimization, two conflicting objectives can be chosen to observe the optimization algorithm's capability to find the Pareto front (a set of parameter sets where none of the metrics can be improved in value without degrading some of the other objective values). Being able to provide DOE or decision makers with a Pareto front will allow them to understand what choices they have for making quantitative improvements in different areas of the fuel cycle, with resulting quantitative degradations in other areas.

The DYMOND/Dakota approach was used to demonstrate some of the powerful analysis capabilities that result from coupling the feature-rich design and analysis kit Dakota to the dynamic NFCS DYMOND. Through the development of this coupling, DYMOND can now be used to identify important design and policy parameters for transition scenarios and how those parameters interact not only with a single response, but also synergistically between all parameters and metrics that may be of interest. This can also be done extremely rapidly with many variations with only a front end computational expense by using previous scenarios to create surrogate models. Though only two surrogate model types and sensitivity analysis capabilities are demonstrated in this study, the coupling is equally functional for the machine learning surrogate model training and model optimization methods available in Dakota. The capabilities demonstrated, and the more advanced capabilities, are not limited to the parameters and responses outlined here. Any arbitrary parameters and responses can be analyzed through this coupling, with up to dozens of each being able to be accommodated in a single study. In the future, these capabilities can be used to develop an efficient multi-level fuel cycle transition optimization framework by down-selecting parameters based on sensitivity values and an iterative optimization of surrogate models used for large parameter spaces, course optimization, and LHS sampling with DYMOND for finer optimization space resolution.

References

Adams *et al.,* 2019   Adams, B.M., Bohnhoff, W.J., Dalbey, K.R., Ebeida, M.S., Eddy, J.P., Eldred, M.S., Geraci, G., Hooper, R.W., Hough, P.D., Hu, K.T., Jakeman, J.D., Khalil, M., Maupin, K.A., Monschke, J.A., Ridgway, E.M., Rushdi, A.A., Stephens, J.A., Swiler, L.P., Vigil, D.M., Wildey, T.M., and Winokur, J.G., "Dakota, A Multilevel Parallel Object-Oriented Framework for Design Optimization, Parameter Estimation, Uncertainty Quantification, and Sensitivity Analysis: Version 6.11 User's Manual," Sandia Technical Report SAND2014-4633, July 2014; updated November 2019.

ANL 2019   H. Thierry, C. Senac, and B. Feng, "DYMOND 6 User Manual," Argonne National Laboratory (2019).

Bae *et al.*, 2019   Jin Whan Bae, Joshua L. Peterson-Droogh, and Kathryn D. Huff. Standardized verification of the Cyclus fuel cycle simulator. *Annals of Nuclear Energy*, 128:288–291, June 2019.

Deb *et al.*, 2002   K. Deb, A. Pratap, S. Agarwal, and T. Meyarivan. A fast and elitist multiobjective genetic algorithm: NSGA-II. *IEEE Transactions on Evolutionary Computation*, 6(2):182–197, April 2002.

DOE 2017   U.S. Department of Energy. (2017). "Advanced Fuel Cycle Cost Basis - 2017 Edition". NTRD-FCO-2017-000265

Djokic *et al.*, 2015   Denia Djokic, Anthony Scopatz, Harris R. Greenberg, Kathryn D. Huff, R. P. Nibbleink, and Massimiliano Fratoni. The Application of CYCLUS to Fuel Cycle Transition Analysis. Technical report, Lawrence Livermore National Lab.(LLNL), Livermore, CA (United States), 2015.

Gidden et al., 2012   Matthew J. Gidden, Paul PH Wilson, Kathryn D. Huff, and Robert W. Carlsen. Once-Through Benchmarks with CYCLUS, a Modular OpenSource Fuel Cycle Simulator. Transactions of the American Nuclear Society, 107:264, 2012.

Huff et al., 2016   Kathryn D. Huff, Matthew J. Gidden, Robert W. Carlsen, Robert R. Flanagan, Meghan B. (ORCID:0000000250213894) McGarry, Arrielle C. Opotowsky, Erich A. Schneider, Anthony M. Scopatz, and Paul P. H. Wilson. Fundamental concepts in the Cyclus nuclear fuel cycle simulation framework. Advances in Engineering Software, 94(C), April 2016.

Ingersoll et al., 2014   D. T. Ingersoll, Z. J. Houghton, R. Bromm, and C. Desportes. NuScale small modular reactor for Co-generation of electricity and water. Desalination, 340:84–93, May 2014.

Kim 2020   S. Kim, PNNL, private communication. 2020.

Kim et al., 2009   T. K. Kim, W. S. Yang, C. Grandy, and R. N. Hill. Core design studies for a 1000mwth Advanced Burner Reactor. Annals of Nuclear Energy, 36(3):331– 336, April 2009.

NRC 2020   "Operating Nuclear Power Reactors." NRC.org, Nuclear Regulatory Commission, Last reviewed 21 Aug. 2020, www.nrc.gov/info-finder/reactors/.

ORNL 2019   Jin Whan Bae, Eva E. Davidson, and Andrew Worrall, "Application of Cyclus to a Transition Scenario," Oak Ridge National Laboratory, ORNL/TM-2019/1286, August 30 (2019). SA&I Campaign FY19 M3 Milestone Report.

Schulez 2006   T. L. Schulz. Westinghouse AP1000 advanced passive plant. Nuclear Engineering and Design, 236(14):1547–1557, August 2006.

Stauff et al., 2015   N. Stauff, E. Hoffman, T. Kim, T. Taiwo. (2015). "Impact of Fast Reactor Technology on Continuous Recycle Fuel Cycle Options in EG23 and EG24". D.O.E Report ANL-FCT-360, Fuel Cycle Research and Development

Variansyah et al., 2020 Ilham Variansyah, Jin Whan Bae, Benjamin R. Betzler, and Germina Ilas. Metaheuristic Optimization Tool. March 1, 2020. https://doi.org/10.2172/1608209.

Wigeland et al., 2014   Wigeland, R., Taiwo, T., Ludewig, H., Todosow, M., Halsey, W., Gehin, J., Jubin, R., Buelt, J., Stockinger, S., Jenni, K., and Oakley, B. (2014). "Nuclear fuel cycle evaluation and screening - final report". D.O.E. Report FCRD-FCO-2014-000106, Fuel Cycle Research and Development.

Appendix A: Cyclus Graphical User Interface

By J. Bae, E. Davidson, and A. Worrall (ORNL)

1   Acknowledgements

2   Introduction

Cyclus [5] is a research system-level fuel cycle simulator developed by universities through multiple Nuclear Energy University Programs (NEUPs). Cyclus is a modular, extensible fuel cycle simulator and was involved in six NEUPs, including one that is currently ongoing. Also, Cyclus is an open source software, facilitating collaboration between multiple universities and institutions by allowing any developer or user to add capability to the Cyclus ecosystem. The Cyclus project is maintained and developed by a voluntary developer team consisting of university faculty, postdoctoral research staff, and graduate students at various institutions. It has been six years since the initial release of Cyclus, and numerous validation studies ([4, 3, 2]) demonstrated Cyclus' competence as a dynamic fuel Fuel Cycle Simulator (FCS).

An examination was completed to identify usability issues of Cyclus, along with a survey of users [1].
The survey identified the following issues:
1. Building and installing Cyclus
     - Cyclus cannot be installed in Windows
     - The binary installation is buggy
     - Building from source is difficult for users unfamiliar with software compiling
     - Numerous dependencies
2. Output parsing
     - Cyclus output is in SQLite format
     - Generates > 20 tables for users to parse through
     - Scripting with knowledge of SQL queries to translate SQLite database to plots / meaningful data
3. Input formation
     - Inconsistent parameter names (e.g. every facility has different names for incoming commodity)
     - Users are unfamiliar with XML structure
4. Outdated documentation

The goal of the project was to design an additional layer of user interface on top of Cyclus. This clarification is important so that the flexibility and openness of Cyclus, which was identified as the biggest strengths of Cyclus, is not harmed. Another design philosophy was to have a guide window for every step, so that a novice user can learn along the way of using the GUI. This then provides an additional objective for the GUI to aid education and learning of the Cyclus tool.

3   GUI Design

To address the identified issues, the GUI is designed to minimize user effort (Fig. 1). The guiding philosophy was to minimize user exposure to Cyclus jargon, and complex 'computer-sciency' tasks such as building software, writing XML, and parsing through an SQL database.
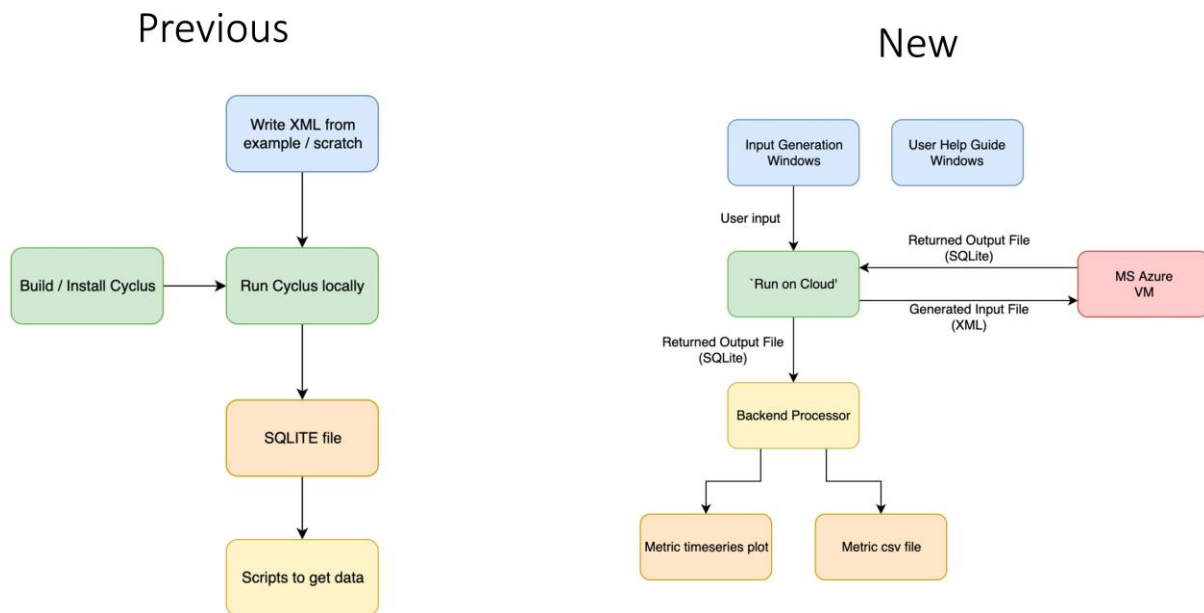
FIGURE 1. The left side shows the previous workflow, and the right side shows the new workflow with the GUI.

3.1   Installation

The application is written in Python, using the GUI package Tkinter. The application is then organized as a Python package, and to standalone executable files. This development flow allows the usage of this application in multiple operating systems (MacOS, Windows, Linux). Also the user simply double-clicks the received application, and does not need to type in complex sequence of commands for installation.
Previously, there were the following methods to install Cyclus:

- Binary installation on Linux (via Debian package or Conda)
- VirtualBox
- Install stable from source (via Tarball or Github Repository)

A lot of the users surveyed were not familiar of these terms, or the methods. Also, some of the methods have been reported as buggy, and depended on the environment (e.g. operating system, installed libraries) the user was in. Alternatively, the developed GUI application is sent to a user in a single .zip file. The user then unzips the file, and double clicks on the executable file, and the application is open. In other words, this GUI application is self-contained.

3.2   Initializing Input

Figure 2 shows the initial window of the GUI. The analysis processes are modular, so that the user has the option to choose where to start from. The user can start from scratch, and follow the left column buttons to create their own input file. Alternatively, input files can be imported from a previous session (using the three letter id), or an existing Cyclus input file. Also, the input file can be initialized to a 'real-life scenario', where the current fleet of countries can be imported from the International Atomic Energy Agency (IAEA) Power Reactor Information System (PRIS) database [6]. The PRIS database lists worldwide reactors with data such as power capacity, reactor type, and build date. The user can select countries to initialize, as well as the year to start from. The user input is used to generate a template using the PRIS database, to generate deployed reactors and their specifications, such as power output, size, and remaining lifetime (Fig. 3). The remaining

lifetime, if not specified in the database, is assumed to be 60 years after the reactors first criticality date. The initialized input files can then be edited in the GUI as well.
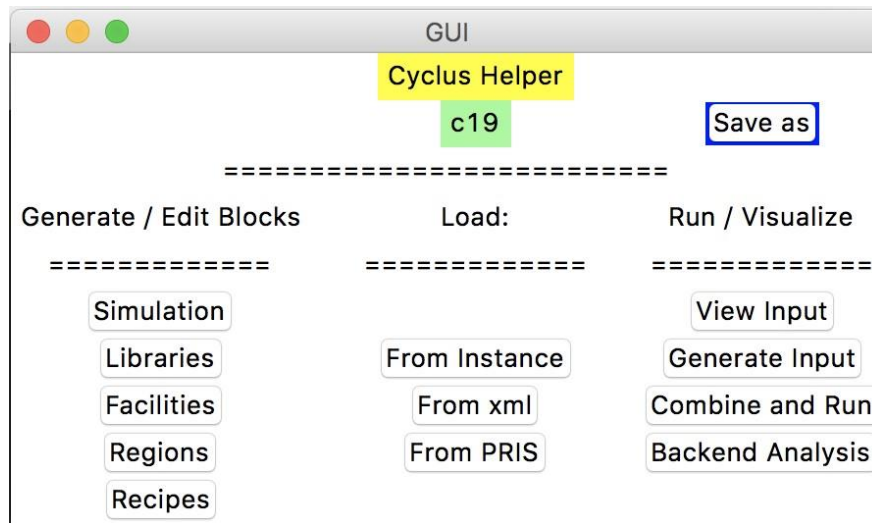

FIGURE 2. The GUI start page. Each session is given a three-letter hash for saving progress. All the files generated in this session are saved to a folder named 'output_c19'.

3.3   Input Generation Windows

There are five input blocks in a Cyclus input: control, archetypes, facility, region, and recipe. The user can create or edit each block from the main menu (Fig. 2). Each button on the main menu generates an input generation window, which guides the user through the input formation of that block. After initialization, the user follows the five buttons to create a full Cyclus input.

The input generation windows are formed to always have an associated guide window integrated, which explains the process at hand, and what it means in a Cyclus simulation. Instead of forming an XML file, the user fills forms that gets rendered to an XML file by the GUI. Throughout the input generation process, a separate status window visualizes the input, by showing defined parameters (Fig. 9). Most parameters and buttons have a mouse hover-over guide text, where the user can see what the button does, or what the parameter means, as well as the input type (e.g. string, Boolean, float).
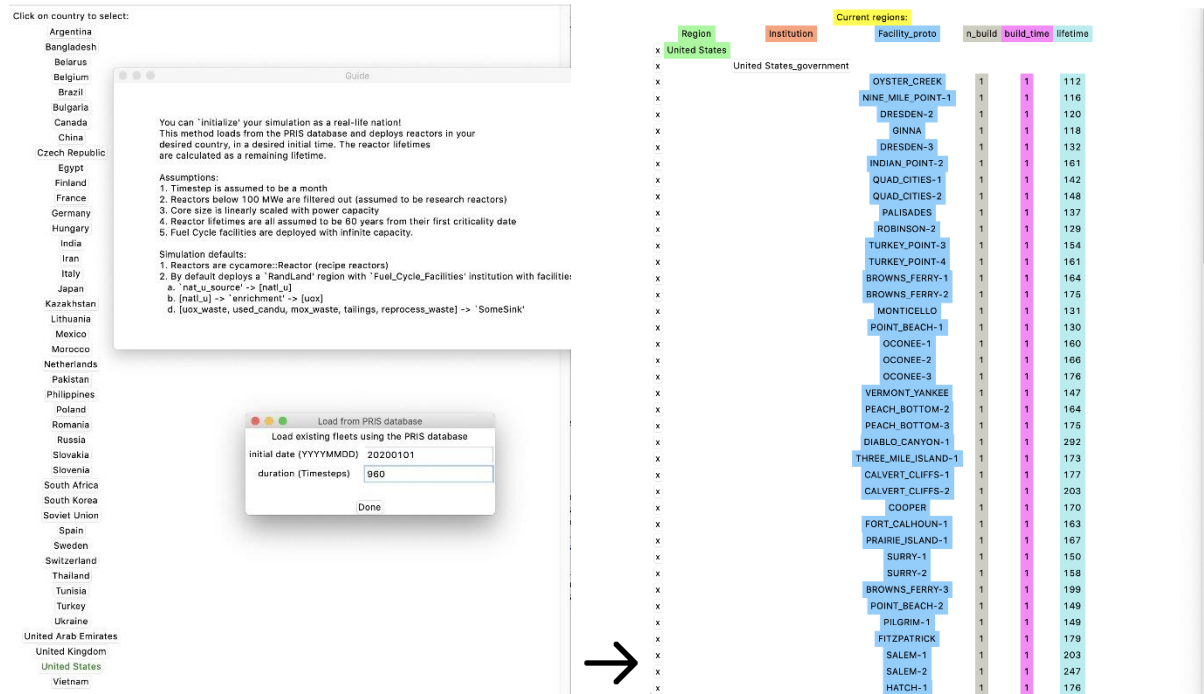
FIGURE 3. This example shows the user selecting United States in 2020 to initialize the simulation from. The GUI generates currently existing U.S. reactors, along with their remaining lifetime in 01/01/2020.
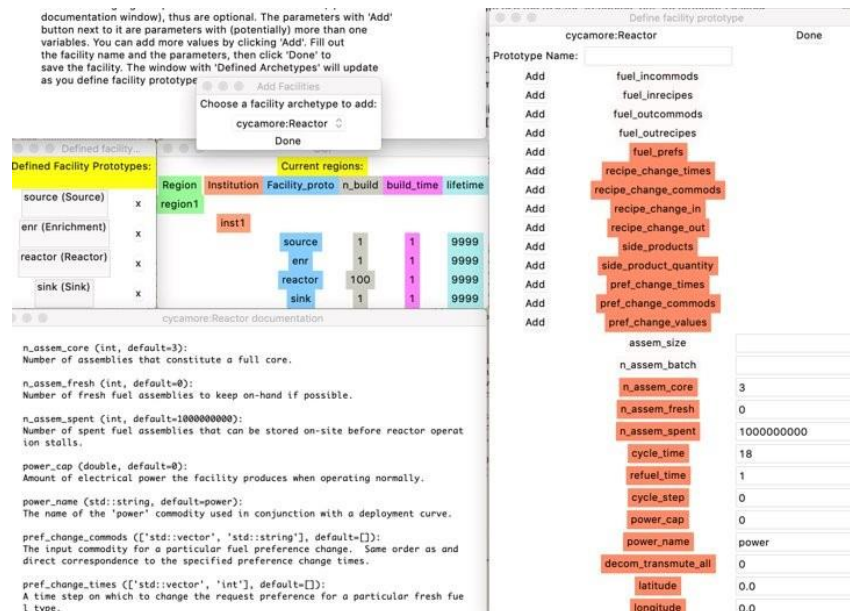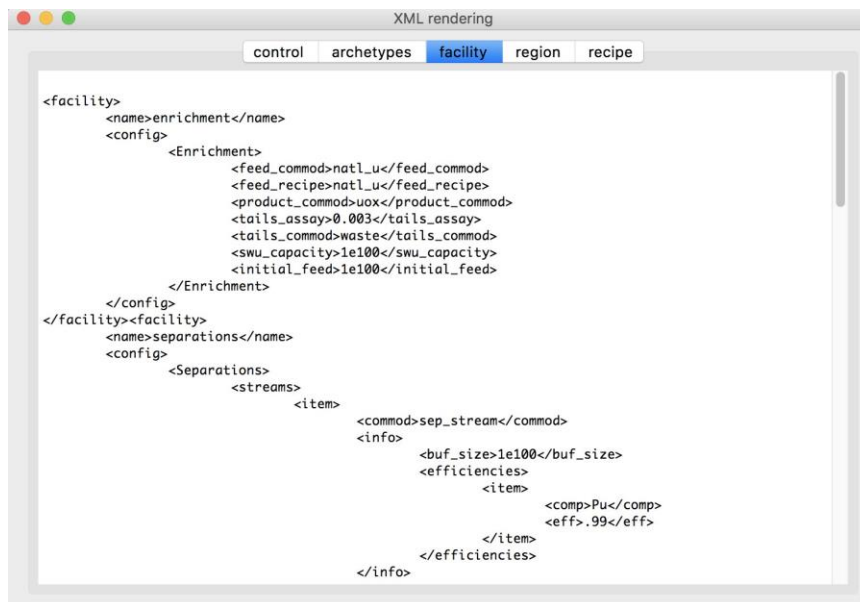
FIGURE 4. Input generation windows in GUI. There are guide windows (upper and lower left) and status windows (middle left) to help the users.

3.4   View Input

Once the input files are formed, the user can see what the rendered XML would look like (Fig. 5). This allows the user to understand how their input is formed into an XML file for Cyclus to read. By doing so, the user can learn about Cyclus input syntax and eventually become expert users of Cyclus.

FIGURE 5. The user can view the rendered XML by the GUI, for educational purposes.

3.5   Run on Cloud

A major usability issue of Cyclus was the difficulty to install Cyclus. As mentioned above, since this GUI is an additional layer, this GUI does not contain Cyclus. Instead, Cyclus is run on the cloud, a separate, central machine that has the most recent stable Cyclus installation. The GUI application only acts as a communicator between the user's local machine and the cloud. By running Cyclus on the cloud, the user does not need to install or build Cyclus on their local machine. Doing so eliminates the need for dependencies and restriction on the Operating Systems (OSs).

In this example (Fig. 6), this functionality connects the user's computer to a pre-configured Microsoft Azure virtual machine, with Cyclus and archetype libraries already installed. In general, this could be any other server (even a laboratory internal server) that has Cyclus pre-installed. There is also an option for the user to use a proxy, for some networks with security restrictions (e.g. national laboratories). The user can also set a password to restrict access. After establishing a successful connection, the GUI will upload the compiled input file (XML) to the cloud server, run Cyclus on the input file in the cloud server, wait for the calculation to finish, and download the completed output file (SQLite) back to the user's local machine. The entire process is piped to the textbox. The textbox also shows debug messages. The user also has the option to run Cyclus locally, if Cyclus is installed in the local machine.
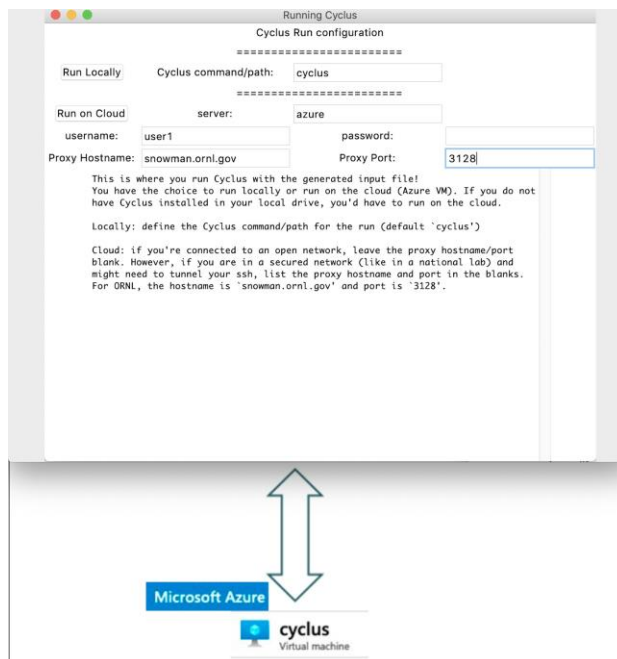
FIGURE 6. Running on Cloud window in the GUI. The box returns any output or error messages from the cloud server.

3.6   Backend Processor

The downloaded output file can be processed by pre-written functions to return metrics and material flows. The GUI has pre-written functions to parse through the SQLite database. This eliminates the need for the user to understand SQL queries and script query results to generate plots (Fig. 7). The GUI also has a function to show material trade between facilities in a network graph (Fig. 8), to visualize the simulation in one plot.

The user can obtain material flow, facility deployment, facility inventory, and Cyclus time series data (Fig. 9). Cyclus time series is a function of Cyclus that allows facilities to record to the database (e.g. Reactor facilities record power generated to the database). Given user input, corresponding data is parsed out from the output SQLite database, and the user has the option to either directly plot or export the data into a comma-separated values (CSV) file.

For plotting, the user can configure the plot settings, such as y axis scale and nuclide notation. The user can also plot / export total mass, or isotopics of the material, by configuring the 'top n isos' parameter.
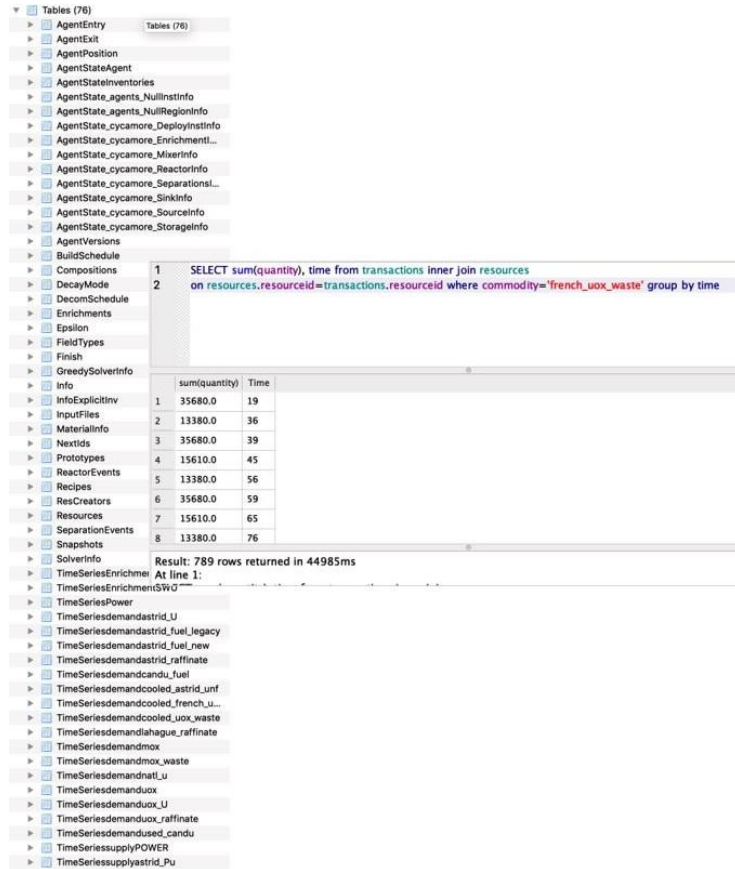
FIGURE 7. Cyclus outputs an SQLite database. To obtain useful metrics and plots, the user would have to understand sql queries as well as the database structure. This need was identified as a usability issue.
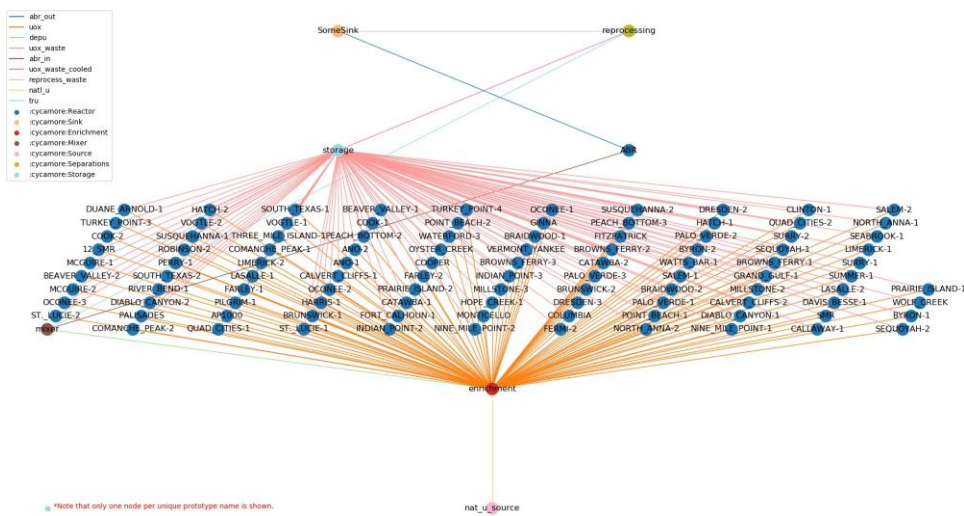

FIGURE 8. This network graph shows an example Cyclus simulation with the existing U.S. fleet. The colors of the nodes denote the type of facility, and colors of the lines denote the commodity traded between them.
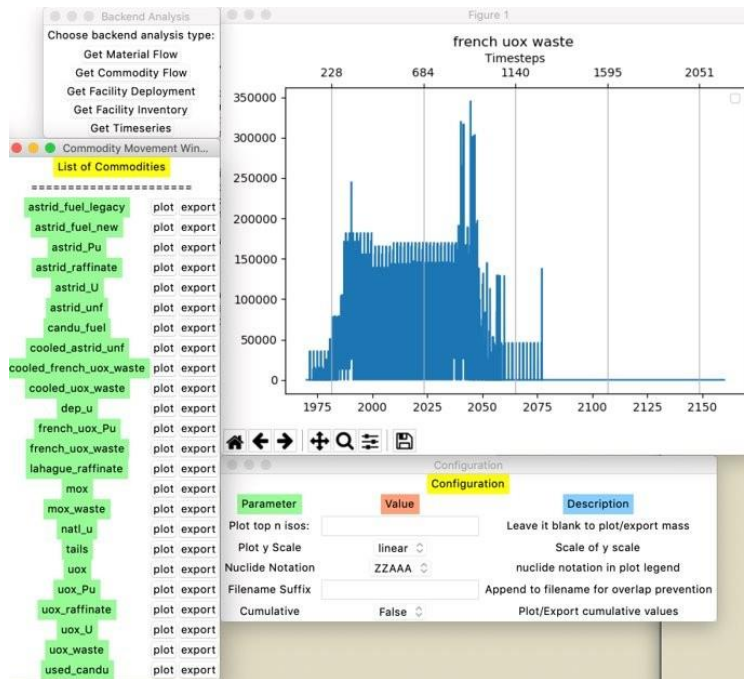
FIGURE 9. The user can now obtain meaningful plots and data without knowledge of SQL queries. The GUI identifies trades in the SQLite database, and provides the user with options.

3.7   Conclusion

The GUI was developed to address the usability issues identified in the survey. The development of the GUI focused on two major points: (1) to not limit the flexibility of Cyclus, while (2) making it easier for novice users to use (and meanwhile learn) Cyclus. This standalone GUI application is easy to distribute and use, and has guide windows to explain Cyclus while users navigate through the application. The GUI is intended to educate the user to understand Cyclus input and concepts, so that they can become expert users later on.

4   Future Work

Another approach to address the usability issue of Cyclus is integrating Cyclus into the Nuclear Engineering Advanced Modeling and Simulation (NEAMS) Workbench application. The NEAMS workbench application is currently used to provide a common user interface for model creation, review, execution, output review, and visualization for integrated codes [7]. Currently, the Argonne Reactor Computation (ARC) suite of codes are integrated into the Workbench.

The main difference between the Workbench approach and the standalone GUI is that the frontend (i.e. generating the input) part of the Workbench is approach is an Integrated Development Environment (IDE), meaning that it is a text editor, where the user gets to write the text input for Cyclus, with autofill, input validation, and templates. This increases the difficulty for the user to generate a Cyclus input relative to the standalone GUI's buttons and fill forms, since there's less room for 'hand-holding' users about Cyclus input structures and what the user needs to define. However, the benefit of using an IDE is that the user using the IDE can learn how to structure a Cyclus input, which allows the user to become expert users later on.
For future work, the goal is to prototype both the Workbench integration and standalone GUI, and have the target users (lab analysts) decide which tool provides the most benefit.

5 **REFERENCES**

[1] Jin Whan Bae, Eva E. Davidson, and Andrew Worrall. Application of Cyclus to a Transition Scenario. Technical Report ORNL/TM-2019/1286, OAK RIDGE NATIONAL LABORATORY, Oak Ridge, TN, United States, August 2019.

[2] Jin Whan Bae, Joshua L. Peterson-Droogh, and Kathryn D. Huff. Standardized verification of the Cyclus fuel cycle simulator. *Annals of Nuclear Energy*, 128:288–291, June 2019.

[3] Denia Djokic, Anthony Scopatz, Harris R. Greenberg, Kathryn D. Huff, R. P. Nibbleink, and Massimiliano Fratoni. The Application of CYCLUS to Fuel Cycle Transition Analysis. Technical report, Lawrence Livermore National Lab.(LLNL), Livermore, CA (United States), 2015.

[4] Matthew J. Gidden, Paul PH Wilson, Kathryn D. Huff, and Robert W. Carlsen. Once-Through Benchmarks with CYCLUS, a Modular Open-Source Fuel Cycle Simulator. *Transactions of the American Nuclear Society*, 107:264, 2012.

[5] Kathryn D. Huff, Matthew J. Gidden, Robert W. Carlsen, Robert R. Flanagan, Meghan B. (OR-CID:0000000250213894) McGarry, Arrielle C. Opotowsky, Erich A. Schneider, Anthony M. Scopatz, and Paul P. H. Wilson. Fundamental concepts in the Cyclus nuclear fuel cycle simulation framework. *Advances in Engineering Software*, 94(C), April 2016.

[6] PRIS IAEA. *Nuclear Power Reactors in the World*. Number 2 in Reference Data Series. IAEA, Vienna, Austria, 2017.

[7] Bradley T. Rearden, Robert A. Lefebvre, Brandon R. Langley, Adam B. Thompson, and Jordan P. Lefebvre. NEAMS workbench 1.0 beta.

Appendix B: Response Metrics of all Scenarios Modeled in DYMOND
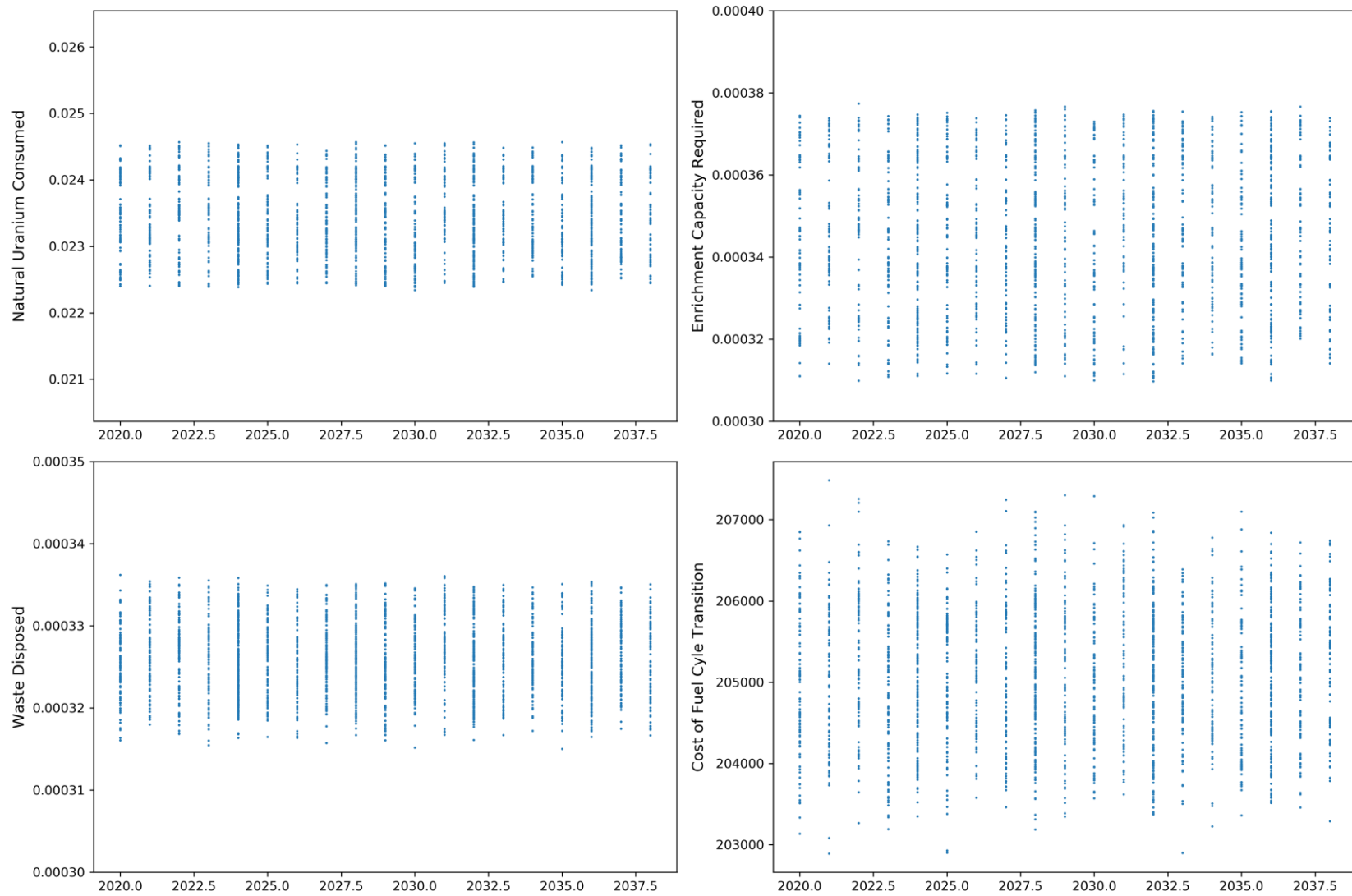

Figure A. 1. Response metric values for sampled values of the start date of the reprocessing facilities.
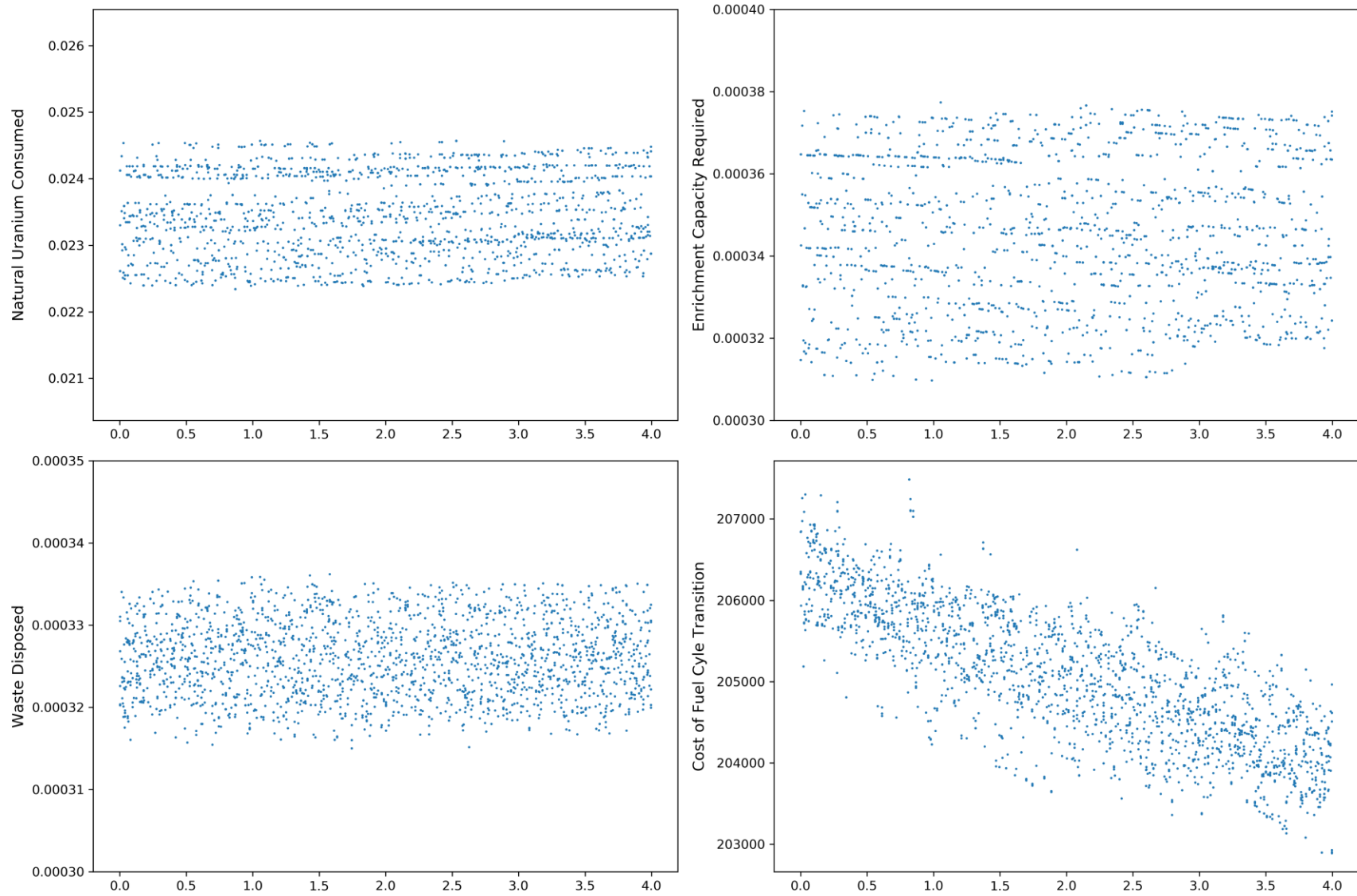
Figure A. 2. Response metric values for sampled values of the scaling factor of the base scenarios' growth in nuclear energy demand.
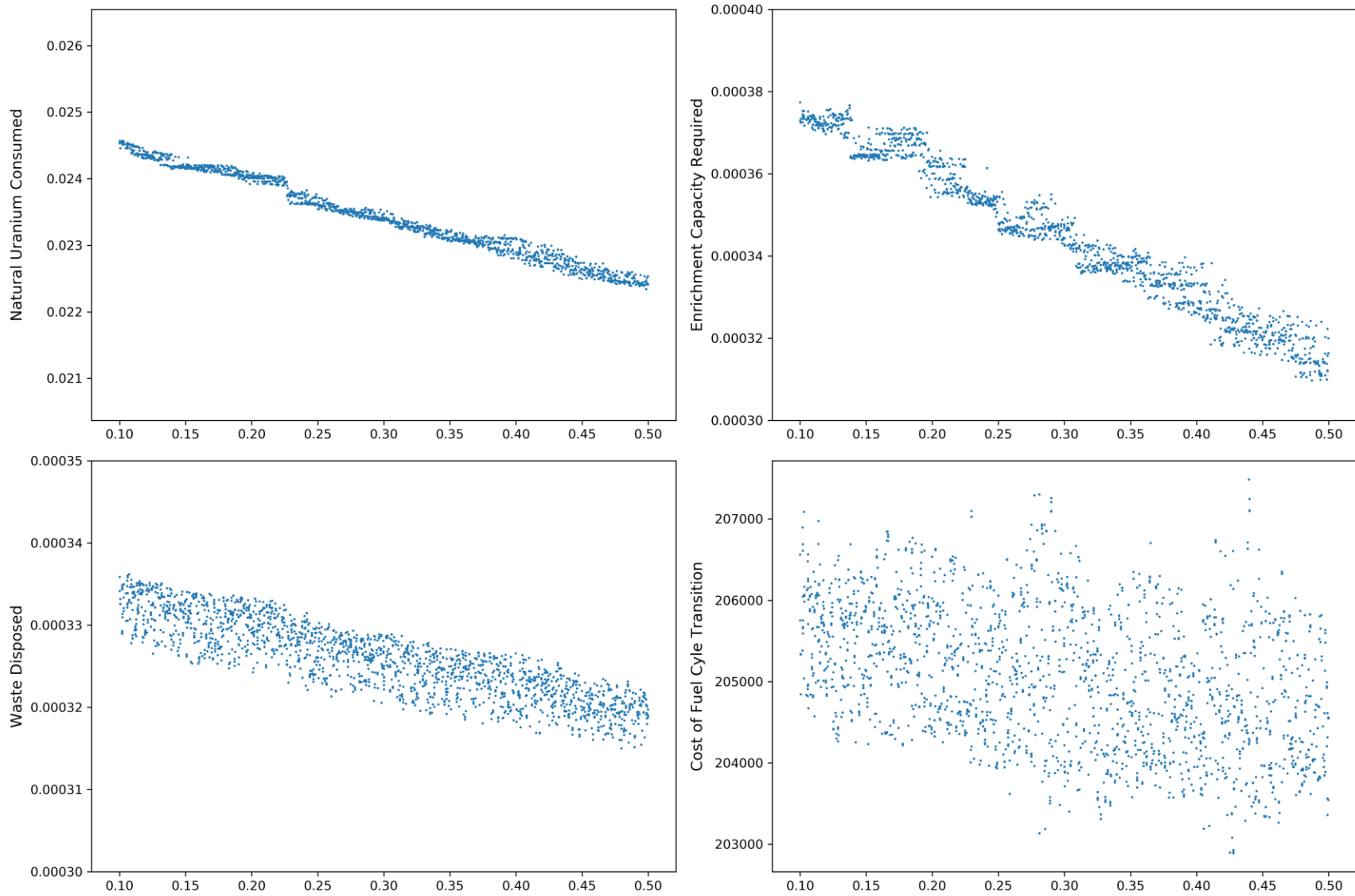
Figure A. 3. Response metric values for sampled values of advanced reactor new build share at the end of simulation.
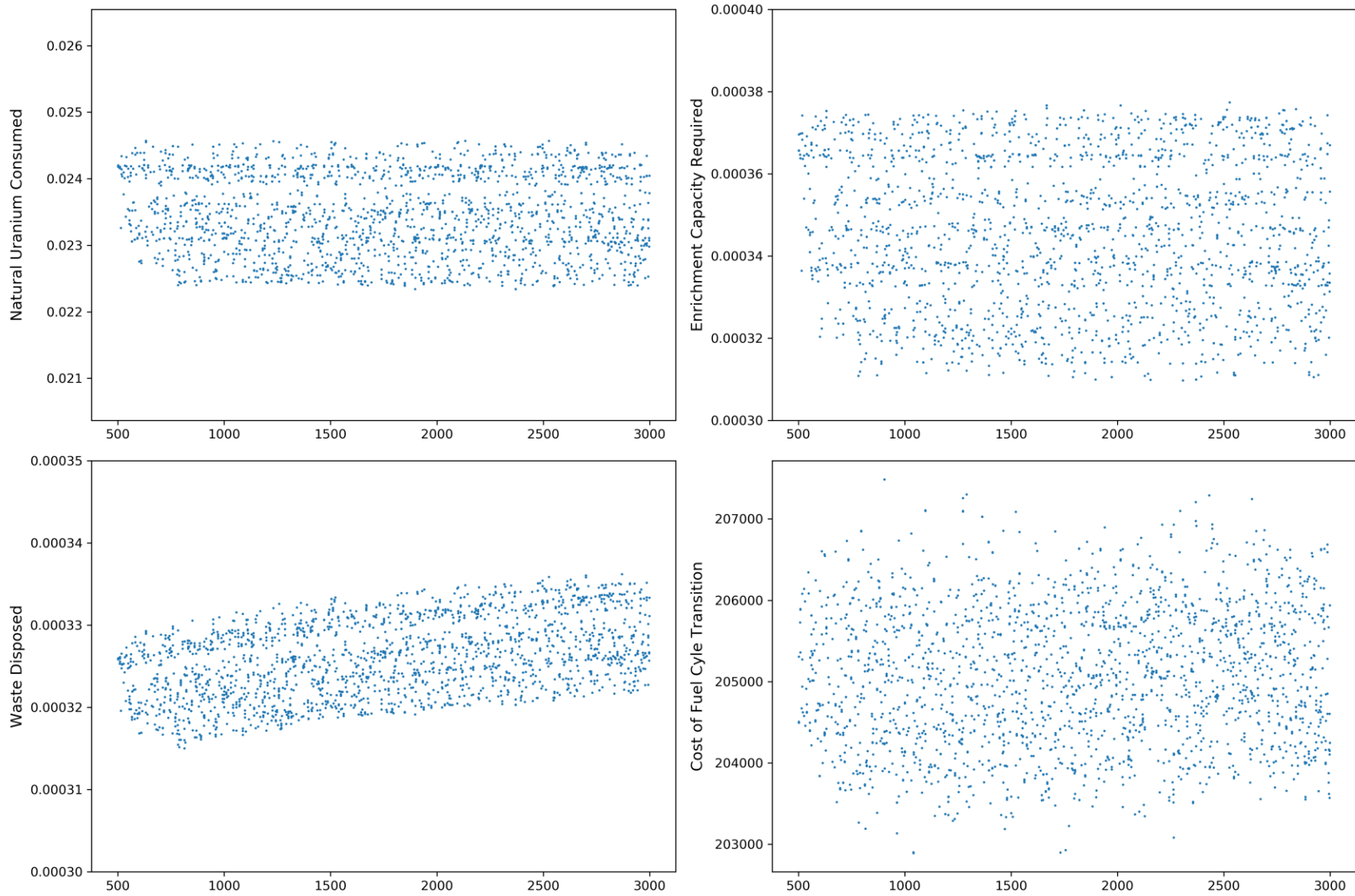
Figure A. 4. Response metric values for sampled values of reprocessing capacity of each of the two facilities

(this page has been left blanket intentionally)